

A Universal Two-Parameter Kratzer-Potential and Its Superiority over Morse's for Calculating and Scaling First-Order Spectroscopic Constants of 300 Diatomic Bonds

Guido Van Hooydonk^{*[a]}

Keywords: Calculations / Bond theory / Electronic structure / Molecular dynamics / Kratzer / Morse / Potential energy curve

After decades of intensive research, the question remains whether or not a universal two- or three-parameter potential exists. For a large number of about 300 bonds, we now critically review the constraints for potentials and asymptotes, involved in three available scaling processes (Varshni, Calder–Ruedenberg, and Graves–Parr). We show that the covalent Sutherland parameter can never be a universal scaling factor. This implies that the usual constraint $U(R) = -D_e$ at $R = \infty$ for potentials is only desirable and that the natural asymptote D_e is not even needed to explain the

relations between the constants. We show that ionic potentials of generalized Kratzer-type (Varshni's V^{th} potential) and their ionic Coulomb-like asymptotes Ae^2/R_e (with A close to 1) behave as simple universal two-parameter potentials. For both α_e and $\omega_e x_e$, this potential gives percentage deviations 2 to 3 times smaller than Morse's three parameter potential for hundreds of bonds. We also prove that the Graves–Parr scaling hypothesis is valid, despite these authors' own conclusion. We discuss various new relations between spectroscopic constants.

1. Introduction

Finding a universal two- or three-parameter potential still has considerable theoretical interest not only for molecular spectroscopy and for the theory of the chemical bond but also for a number of practical chemical processes such as metallic adhesion, cohesion and chemisorption, where similar potentials appear.^[1]

For decades, considerable efforts were made on scaling potentials and/or spectroscopic constants.^[1–15] This ever-continuing search for what Tellinghuisen^[10] once called the *Holy Grail of Spectroscopy* remains justified since the spec-

troscopic constants of a large number of diatomic bonds exhibit an extremely simple, intriguing behavior, not yet accounted for theoretically. Various opinions persist whether or not a universal low parameter function really exists and the matter is certainly not yet solved.^[9] Experience shows that even a three-parameter potential cannot be of universal character,^{[2][3]} a thesis we will now reconsider.

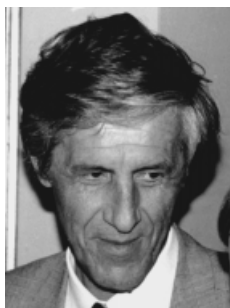
In this review, we use a method devoid of two of the common problems in this kind of research, e.g. finding representative sets for

(a) *molecules (and constants)*: the set used here is beyond doubt representative and also large enough, as we collected all readily available spectroscopic data for about 400 bonds and for

(b) *potentials*: here we confront two completely different low-parameter reduced potentials: a reputed covalent one and a less known ionic one. Both stand for a series of related potentials in their category.

^[a] Ghent University, Department of Library Sciences, and Department of Physical and Inorganic Chemistry, Rozier 9, B-9000 Ghent, Belgium
E-mail: guido.vanhooydonk@rug.ac.be

Supporting information for this article is available on the WWW under <http://www.wiley-vch.de/home/eurjoc> or from the author.



The author (born 1944) obtained his Ph.D. in 1971 at the University of Ghent (chemistry). He then moved to the University Library, built in 1935 by the famous Bauhaus co-founder, designer and architect Henry Van de Velde. – In 1990 he became professor and chief librarian. He implemented an integrated library system, one of the first in Europe to focus on a dynamic integration of bibliographic sources with the on-line catalog (<http://www.lib.rug.ac.be>). He published books and articles on different aspects of the library and on a derivative of library sciences, bibliometrics. – Since 1971, he published about 40 articles on many aspects of the theory of the chemical bond, still his main research interest. Numerous spectroscopic data are used to confront bonding theories with experiment. Recent experimental work is on the analysis of pigments in medieval manuscripts by TXRF- and micro-Raman spectrometry. Prof. Van Hooydonk is a referee for many journals and a member of national and international societies in exact and in library sciences.

MICROREVIEWS: This feature introduces the readers to the authors' research through a concise overview of the selected topic. Reference to important work from others in the field is included.

2. Overview of Scaling Spectroscopic Constants and Potentials: Aim of This Work

The most essential (zeroth order) information about chemical bonding is contained in only *three constants*: the dissociation energy D_e (the natural asymptote), the bond length R_e and the force constant k_e . These determine an important *species-dependent* scale factor, the dimensionless Sutherland^[11] parameter Δ , defined as

$$\Delta = 1/2 k_e R_e^2 / D_e = a_0 / D_e \quad (1)$$

Herein a_0 , the first coefficient in the Dunham expansion^[12] near the minimum and representing the asymptote in the harmonic oscillator presentation, is scaled by D_e , the atomic dissociation limit or the natural asymptote. By definition, a_0 is determined by the two zeroth order spectroscopic constants (see below). D_e can be determined experimentally in various ways.

For the two *first order spectroscopic constants*, Varshni^[3] introduced two dimensionless parameters F and G also related to the next coefficients a_1 and a_2 in the Dunham expansion. Both F and G derive from the potential and are numerical functions of Δ . From these two theoretical relations $F(\Delta)$ and $G(\Delta)$, a theoretical $G(F)$ relation follows. The experimental $G(F)$ plot is, in general, roughly in line with the theoretical expectations for empirical potentials.^[6] Many inconsistencies, almost like a “spectroscopic gap” between different kinds of bonds,^[6] are found both in $F(\Delta)$ - and $G(\Delta)$ plots, *meaning that something fundamental must be wrong with the Sutherland parameter as a scaling aid in molecular spectroscopy*.^{[3][6]}

Although 30 years after Varshni's standard analysis^[3] of 23 bonds, Graves and Parr^[2] analyzed 150 bonds and argued that the square root of the Sutherland parameter is the better species-dependent scale factor, this new scaling operation did not fit the experimental data any better.^[10] Both the Varshni and the Graves and Parr analyses are essentially similar and lead to the same conclusions. Scaling by the Sutherland parameter (Δ or even $\Delta^{1/2}$) is not effective, which is correct. Their next conclusion that, therefore, a universal three-parameter potential cannot exist, is probably not correct, as we intend to demonstrate in this study and did so already some time ago on a smaller scale.^{[6][7]}

Later, Jhung and co-workers^[9] proved theoretically that a universal three-parameter function exists, but, unfortunately enough, they were unable to identify its analytical form. The best candidate, to their opinion, would be the Morse potential.^[13] However, this popular (overworked^[3]) potential is known to be bad for ionic bonds, a class of molecules not studied by Jhung.^[9] Smith et al.^[14] suggested to include an ionic term in the potential, a procedure that gave good results.

Graves and Parr in their analysis of the scaling problem^[2] concluded that a three-parameter potential must always make some compromise on D_e , R_e , or k_e . This seems like an invitation to question the universal character of Δ , where these three constants are united, see Equation (1). Looking

for such a compromise is one of the challenges of this work. In fact, we suggested some time ago,^[6] even before Graves and Parr, that an alternative Sutherland parameter should be used and that a universal potential might be of ionic type, an hypothesis to be reviewed now in the context of scaling on a much larger set of bonds.

This thesis is in line with the alternative scaling (Sutherland-like) parameter t , introduced for ionic bonds by Varshni and Shukla^[4] many years ago and used by Van Hooydonk^[6] as a universal scaling parameter for both ionic and non-ionic bonds. Ionic potentials^[4] use an asymptote D_x , different from D_e , leading to an alternative Sutherland parameter a_0/D_x . This shift in asymptotes seems a solution for the compromise, suggested by Graves and Parr.^[2]

Recently, and in line with our earlier work,^[6] also Von Szentpaly^[15] suggested another alternative asymptote D_x : the valence state energies of the atoms, which refers to a rather classical Atoms In Molecules (AIM) approach. This asymptote consists of two separated atoms, frozen in the same valence state they have at the equilibrium distance. In this terminology, an ionic approach is an IIM (Ions In Molecules) method, which freezes ions instead of atoms. Both our results with the IIM method^[6] and Von Szentpaly's with AIM method^[15] remove several problems with $F(\Delta)$ - and $G(\Delta)$ plots, due to the use of the covalent Sutherland parameter.

Very recently and partly because of these latter two approaches, Freeman, March, and Von Szentpaly^[16] argued that an empirical power relation between G and F would be evidence for chaotic/fractal behavior in anharmonicities. As one can never underestimate the impact of (inverse-) power-laws, such as Coulomb's, in chemistry and physics, this problem is now reviewed also.

We now collected constants of 400 diatomic (*inorganic*) molecules, with bonds between zero-, mono-, and polyvalent atoms, of molecular ions, of isotopomers, and of excited states. Scaling based upon alternative asymptotes and simple potentials is critically examined by three related scaling methods available in the literature (Varshni,^[3] Graves–Parr,^[2] and Calder–Ruedenberg^[5]).

Except for the data collection (section 3), the paper is divided in 4 main sections: (4) theoretical constraints for potentials; (5) extensions and consequences of earlier results on scaling properties of the covalent Sutherland parameter; (6) the search for a universal two-parameter function: theoretical requirements and (7) the search for a universal two-parameter function: testing the theoretical results with the constants.

3. Data Collection

Data for 402 bonds are taken from Huber and Herzberg^[17] and Radzig and Smirnov,^[18] without checking for accuracy. Different mass units are used ($C = 12$ in the first and a.m.u. in the second). For 21 bonds, first order constants are not simultaneously available. For 76 bonds, D_e is not available, which leaves about 300 bonds for a one-by-

one comparison between covalent and other scaling approaches.

4. Theoretical Constraints for Potentials

4.1 Universality of Potentials

Two methods can be used to decide whether or not a function is universal: (a) PECs, potential energy curves (RKR method) fall within $\pm 5\%$, of the function and/or (b) calculated spectroscopic constants fall $\pm 5\%$, of the experimental values. In either case, the number of a variety of bonds must be large. Method (a) can be used in combination with (b). However, since the number of bonds in this study is very large, we can only use method (b). A perfect result for (b) does not warrant the same result for (a) in the complete range $0 \leq R \leq \infty$ (Steele et al.^[8]).

4.2 The Dunham Expansion

The Dunham expansion^[12] around the minimum is:

$$U(\rho) = a_0 \rho^2 (1 + a_1 \rho + a_2 \rho^2 + \dots) - D_e \quad (2a)$$

where a_n are constants and where the variable is

$$\rho = (R - R_e)/R_e \quad (2b)$$

The first term is the well-known harmonic oscillator equation and the first constant (the well depth or the Dunham asymptote) is given by [see also Equation (1)]:

$$a_0 = \omega_e^2/4 B_e \quad (2c)$$

Since a_0 is solely determined by zeroth order spectroscopic constants, the Dunham asymptote is a *mathematical* asymptote. The next Dunham coefficients are related to the first-order constants: a_1 to a_e , the rotation-vibration constant, and a_2 to $\omega_e x_e$, the anharmonicity constant. Dividing all terms in (2a) by D_e shows why the covalent Sutherland parameter is an important scaling aid. Conversely, accounting for the higher Dunham coefficients is also a major test for the universal character of a potential.

4.3 Constraints for Potentials and Asymptotes

Although constraints for potentials can be divided in two classes: necessary and desirable (Varshni^[3]), we will restrict ourselves here to some general constraints. As remarked by Von Szentpaly,^[15] one global constraint is that an A/R^x -law is preferential for *attraction*

– A should allow for interacting charges: the concept of *valences* (as in the Calder–Ruedenberg Column classification,^[5] also used by Graves and Parr^[2]), for *charge-transfer* between partially charged atoms, as argued by Smith, Schlosser, Leaf, Ferrante, and Rose^[14]

– $1/R^x$ should allow for the idea of forces *getting smaller with distance* (reflected in

the Herschbach and Laurie Row classification^[19])

(a) with $x = 1$, this is in line with *Coulomb's fundamental law*, and in the next instance, with ionic bonding (see Berzelius,^[20] Kossel,^[21] Van Hooydonk^[6]), although also covalent bonding calls for a $1/R$ -law (Borkman and Parr,^[22] Sanderson^[23])

(b) with $x \neq 1$, a number of other possibilities are open (Varshni^[3]), among which the idea of (inverse) *power-laws* (see Freeman, March and Von Szentpaly^[16]).

For *repulsion*, a large number of solutions are available (see Varshni^[3] for a review).

More detailed constraints for potentials are not repeated here (see for instance Varshni,^[3] Calder and Ruedenberg,^[5] Jenc^[8]). Basic constraints for any potential $U(R)$ are

(i) $U(0) = \infty$ (or very large) and $U(\infty) = 0$

(ii) $U(R_e) = -D_e$

(iii) $U'(R_e) = 0$ and

(iv) $U''(R_e) = 4\pi^2\mu\omega_e^2 = k_e$ (the force constant or the curvature at the minimum), where μ is the reduced mass. The force constant and R_e determine the first coefficient in the Dunham expansion a_0 , see Equation (1) and (2c). Replacing condition (ii) by $U(R_e) = -D_x$ instead of D_e does not alter any of the next mathematical steps required to arrive at Varshni's parameters F and G . Scaling the higher derivatives $U'''(R_e)$, $U^{IV}(R_e)$, ... by the force constant $k_e = U''(R_e)$, leads the parameters X and Y , related to F and G and to the next coefficients in the Dunham expansion a_1 and a_2 and to the first order constants. At this stage, Sutherland's parameter comes in as a scaling factor, called so by Varshni^[3] to honor Sutherland's work.

The question is whether constraint (ii) is either necessary or only desirable. We know of no simple (low parameter) analytical function that accounts for the atomic dissociation limit, whereas a large number of simple analytic potentials are available, leading to well defined but different asymptotes. Also Von Szentpaly^[15] gave arguments for replacing the atomic dissociation limit as a scaling factor and retraced earlier arguments to do so (see also below). We will consider constraint (ii) as *desirable*, since exactly this condition expresses our *desires* and expectations about a perfect universal function. Modifying constraint (ii) is also a way of interpreting the empirical fact that, after decades of intensive research by numerous researchers all over the world, a really universal (low parameter) function has not yet been found.

All other constraints mentioned above *must remain valid* for a universal function (mainly for reasons of *internal consistency*). However, if *any* two or three-parameter function can be found that produces an asymptote D_x with a simple chemical meaning and which scales the Dunham coefficients efficiently, the question of scaling is probably solved. How to reach the atomic dissociation limit with that potential, would lead to a different, more transparent, situation.

The Dunham expansion itself does not require the atomic dissociation limit. It is limited to the situation around the equilibrium internuclear distance in the first place and to a consistent reproduction of the spectroscopic constants by

means of a relatively simple series expansion in terms of an harmonic oscillator model (see below).

5. Previous Results on the Scaling Properties of the Sutherland Parameter

5.1 The Zeroth Order Spectroscopic Constants (the Dunham Asymptote) and Scaling

Scaling has much to do with the relations between the constants determining a_0 , as scaling is essentially a two-dimensional operation (Graves and Parr^[2]).

The two zeroth order constants (the vibrational constant ω_e and the rotational constant B_e) are known to have a very intimate relationship, which made $1/R$ potentials so popular in the past, since $B_e = 1/(\mu R_e^2)^{1/2}$.

An $\omega_e(B_e)$ plot shows two basic characteristics: (a) a Row dependency (Herschbach–Laurie^[19]) and (b) a Column dependency (Calder–Ruedenberg^[5]).

Figure 1a on the Row dependency and Figure 1b on the Column dependency represent some of the results obtained from our data. The almost parallel lines combining molecules in the same Row have an intercept at the x -axis (B_e), whereas the parallel lines representing the Column classification have an intercept at the y -axis (ω_e). Taking two parallel lines in Figure 1b (Column dependency) together with two parallel lines in Figure 1a (Row dependency) would always result in a (scaled and oblique) replica of the Periodic Table. A similar scattering is observed when a plot (not shown) is made for the two first order constants: $\omega_e x_e$ (or x_e) and α_e . Figure 1c gives the normal (i.e. non-logarithmic) plot between the two zeroth order constants.

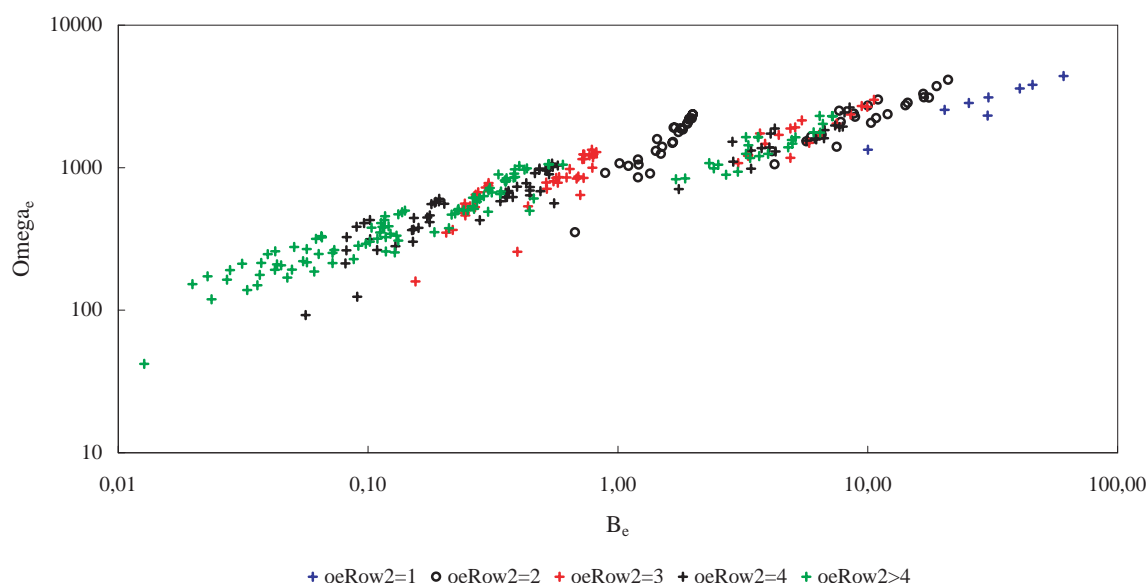


Figure 1a. Ω_e versus B_e for 300 bonds (Row-classification) (log-scale)

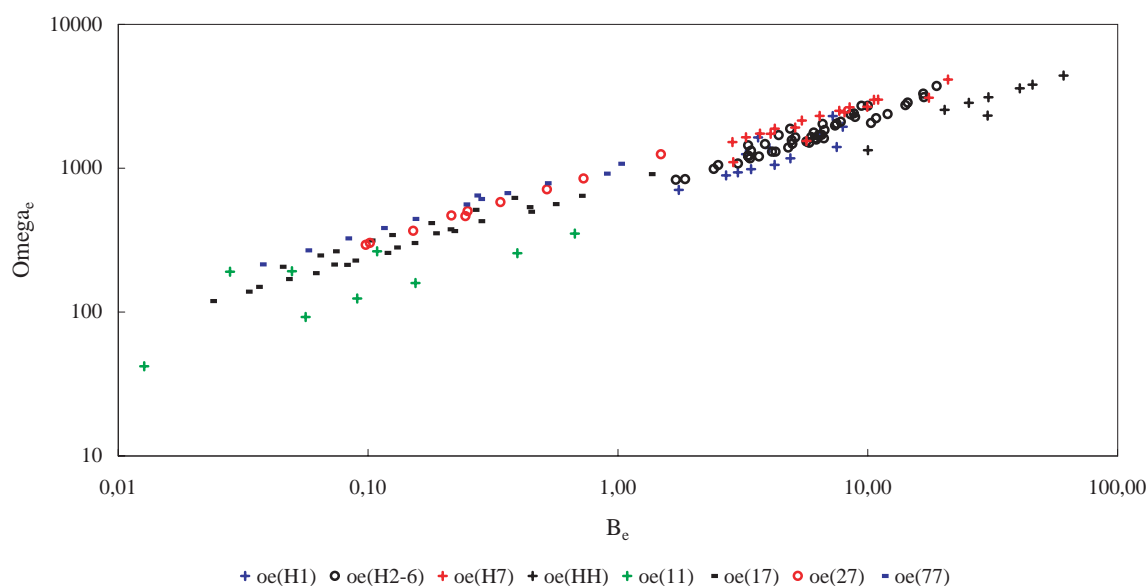


Figure 1b. Ω_e versus B_e for 300 bonds (Column-classification) (log-scale)

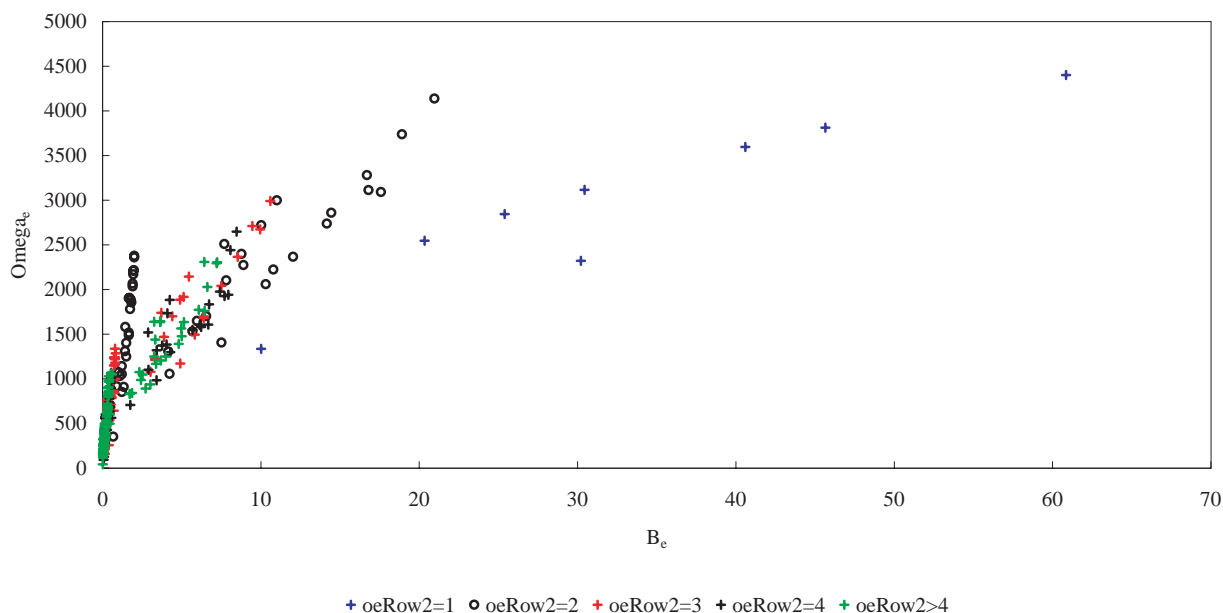


Figure 1c. Ω_e versus B_e (Row-classification) (normal scale)

Perfect scaling seems to consist in reducing these replicas of the two-dimensional table to a one-dimensional version. For *atomic spectroscopy*, this would not be a problem, since either the atomic number Z or the atom mass M can be used (both are rather simply related to one another). The H atom is the prototype in atomic bonding: its energy and its spectroscopic behavior are easily computed from first principles. But, if perfect scaling in *molecular spectroscopy* can be achieved, a similar solution must exist: using first principles, a universal potential will determine the energy and the spectroscopic behavior of a universal bond, which can then be considered as the equivalent of the H atom in atomic spectroscopy. To arrive at a situation analogous to that found in atomic spectroscopy, a scaling system must be found which brings the scattering in the data-points in Figure 1a–c down to almost a single smooth line.

Since the two zeroth order constants completely determine the Dunham asymptote, such a relation would be extremely valuable for scaling this asymptote. In second order, scaling a_0 has immediate consequences for the first order constants also, according to Varshni's analysis^[3] and its Graves–Parr variant.^[2] Despite the fact that a $1/R$ law seems to interfere with the two constants that determine a_0 , scaling the Dunham asymptote is almost invariably done by means of D_e , the atomic dissociation limit (the covalent Sutherland parameter).

5.2 Relations Between First-Order Constants (Varshni Functions F and G) and Scaling by the Covalent Sutherland Parameter: Early Observations

In addition to a re-appraisal of the Sutherland parameter, Varshni^[3] showed that two dimensionless parameters F and G relate to the first order spectroscopic constants:

$$F = a_e \omega_e / 6 B_e^2 \quad (3)$$

$$G = \omega_e x_e \mu R_e^2 / 2.1078 \cdot 10^{-10} \quad (4)$$

However, already 40 years ago, Varshni remarked that $F(\Delta)$ - and $G(\Delta)$ plots for 23 bonds seemed to generate two sets of different molecules, for which he could hardly give an explanation.^[3] Therefore, he *had* to conclude that a universal three-parameter potential probably could not exist. Varshni's early observation was later referred to as a *spectroscopic gap*^[6] between different types of bonds as it leads to a conflict between the Morse potential and the covalent Sutherland parameter. In fact, we now made a plot (see Figure 2a) of the Varshni function F (related to a_1) against the square root of the covalent Δ for 91 bonds between monovalent atoms. The theoretical result^[3] of a Morse potential is $F = \Delta^{1/2} - 1$ and is represented by a solid line in Figure 2a. If the Morse potential is the most likely candidate for being a universal function (Jhung et al.^[9]) and if $\Delta^{1/2}$ is the best scaling factor (Graves and Parr^[2]), something very elementary must be wrong: only 22 out of 91 data-points (25%) are on or close to the line theoretically predicted by the Morse potential.

To make things worse, a $G(\Delta)$ plot leads to the same situation (Varshni,^[3] Van Hooydonk^[6]). In this case,^[3] the Morse potential predicts that $G = 8\Delta$. Figure 2b gives the corresponding plot for the same 91 bonds. We can only conclude again either (a) that the Morse potential can never reach the status of a universal potential or (b) that the covalent Sutherland parameter can never be a perfect universal scaling aid.

Strangely enough, most of these discrepancies disappear when G is plotted directly as a function of F , whereby the intermediary step involving the covalent Sutherland parameter Δ is avoided. This illustrates the intriguing relations,

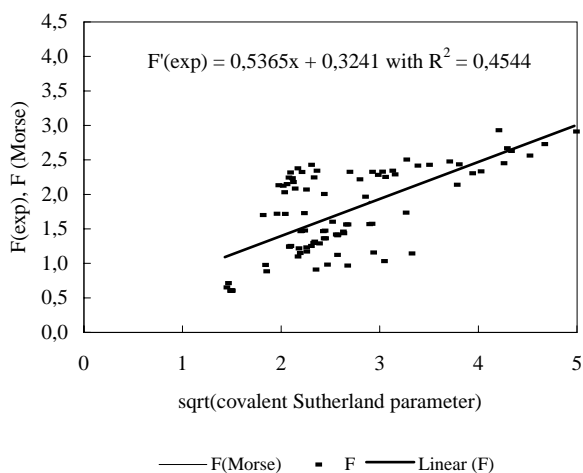


Figure 2a. $F(\text{exp})$ and $F(\text{Morse})$ versus $\text{sqrt}(\text{covalent Sutherland parameter})$ for 91 single bonded diatomics

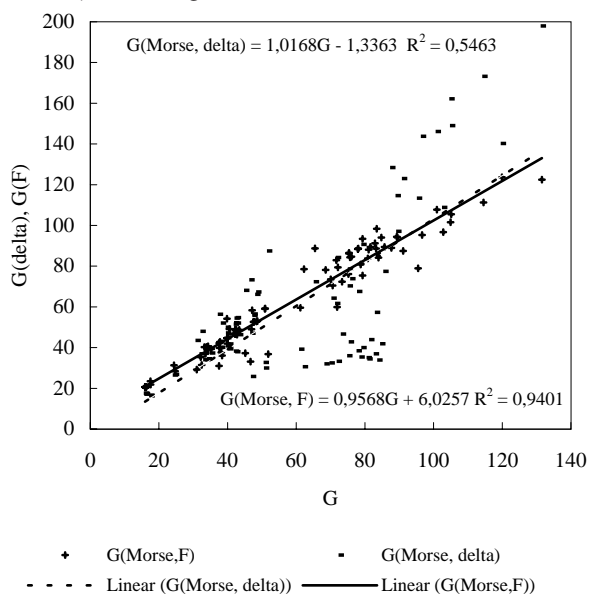


Figure 2b. $G(\text{Morse, delta})$ and $G(\text{Morse, F})$ versus G for 91 single bonded diatomics

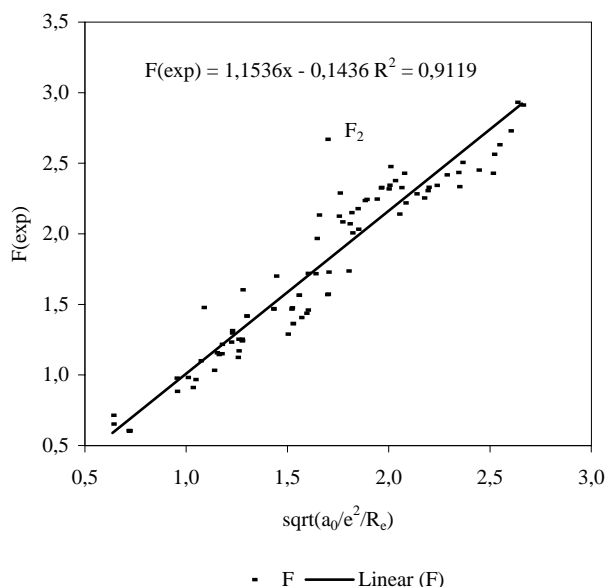


Figure 2c. $F(\text{exp})$ versus $\text{sqrt}(a_0/e^2/R_e)$ for 91 single bonded diatomics

that exist between the spectroscopic constants and shows that, in reality, there is no spectroscopic gap at all.^[6]

This effect is also shown in Figure 2b by the data-group $G(\text{Morse } F)$. If we use the prediction of the Morse potential that $\Delta = (1 + F)^2$ and calculate G from $G = 8(1 + F)^2$, i.e. without the interference of Δ values, the Morse's three-parameter potential almost behaves like a universal function (Jhung^[9]).

Consequently, the covalent Sutherland parameter is not at all a good scaling factor. This answers our dissatisfaction with the last conclusion by Varshni^[3] and Graves and Parr^[2] that a universal *three*-parameter potential (like Morse's) does not exist, if this conclusion is based on the fact that scaling with the covalent Sutherland parameter does not work.

We see that things go wrong as soon as an external parameter D_e , not simply related to the zeroth order constants, is introduced as a scaling parameter for a_0 , which is completely and solely determined by these zeroth order constants. And although attempts were made to correlate D_e with some constants, such a correlation has no universal validity (probably on account of the very same reason: we refer to the linear Birge–Spooner extrapolation, discussed by Varshni,^[3] which is ultimately also based upon the usefulness of a covalent Δ for scaling).

It appears that F and G would both be independent of D_e . The Morse potential is not a universal potential in the whole range of R values (0 to ∞) but appears to be a good approximation to a universal function around R_e . This is not a surprise, when one looks at the analytical form of and the variable in the Morse function: both are very similar to Dunham's.

5.3 An Alternative Sutherland Parameter

Having to re-scale Δ , the most important species dependent scaling factor in molecular spectroscopy, may seem a drastic measure. We discuss the two asymptotes involved.

5.3.1 The Dunham Asymptote a_0

This mathematical asymptote is determined by the zeroth order constants alone. Hence, only mathematical re-scaling can be allowed. At least theoretically, re-scaling the Dunham asymptote is not that strange after all, since Dunham used the variable $(R - R_e)/R_e$ in his harmonic oscillator model.^[12] For small deviations around the equilibrium distance, this variable refers to energies varying with R , which is not in line with observation on the molecular level and in physics and chemistry. The resulting well depth a_0 is difficult to understand in terms of a bonding model and it always leads to a completely wrong and too large a dissociation limit at $R = \infty$. This asymptote is not a natural atomic or molecular state but a mathematical artifact. It results from forcing Hooke's law to apply to chemical bonding, in an attempt to recover mathematically all lower order spectroscopic constants in the harmonic oscillator

model. However, *this limitation of Dunham's asymptote is at the same time also its major advantage*: it provides us with a true, i.e. mathematical, reflection of the situation at the minimum, without any interference of external or higher order effects.

Now, the very similar variable $(R - R_e)/R$ would almost give the same oscillator behavior around R_e . In addition, this variable refers to an attractive energy varying with $1/R$, much more plausible in physical and chemical processes and the potential would not behave badly at $R = \infty$, as it will always converge to a finite limit (Van Hooydonk;^[7] Simons, Parr, and Finlan^[24]). This variable is well-known in physics and chemistry and was introduced by Kratzer,^[25] more than 10 years before Dunham published his analysis.

The mathematical re-scaling for a_0 consists in a change of variable in Dunham's series. A change in the variable has a consequence for the asymptote, equal to

$$D_x = D_{\text{ion}} = e^2/R_e$$

corresponding with an (ionic) Coulomb energy between two point charges (attraction through a $1/R$ -law) and with an ionic bonding model. Experiment shows that very often $D_e < D_x < a_0$, which is important for other reasons (see below). For 40 bonds, the performance of Kratzer potentials is good, even for higher order spectroscopic constants,^{[6][7]} not under review now.

5.3.2 The Atomic Dissociation Limit D_e

Like constraint (ii), this limit seems untouchable, as it is experimentally and consistently reproduced in various ways. Yet, it is not closely bound to the low order constants as is a_0 at $R = R_e$.

Indeed, a number of effects can interfere between R_e and ∞ before the atomic dissociation limit is actually reached (see Varshni^[3]). We give two examples. First, if the non-crossing rule interferes between the minimum and ∞ , a fundamental change in the potential or in its parameters must have occurred. Consequently, the atomic dissociation limit D_e is then not a true reflection of the bonding situation at R_e (Varshni^[3]). Second, if the atoms are *charged* at R_e , as in ionic bonds, a dissociation into *neutral* atoms is not a true reflection of the bonding state either. However, these two disturbing situations can never occur for the (artificial) Dunham-dissociation process, leading to a_0 , which is, by definition, always and only, a true reflection of the bonding characteristics at R_e . If in some cases the atomic dissociation limit D_e is an n^{th} order asymptote, it has been subjected to effects, which are not included in the zeroth order potential describing the situation at the minimum. Then, we are in need of another alternative asymptote (and potential) that can be used to scale a_0 accordingly.

5.3.3 Constraints for an Alternative Sutherland Parameter

A possible solution would consist in leaving out the atomic dissociation limit as a scaling energy-level and a

change of the variable in the Dunham potential, which entrains a different asymptote automatically (an ionic one in the case of the Kratzer variable).

The *necessary* constraints for an alternative asymptote D_x remain stringent: it should

- have a simple relation with zeroth order spectroscopic constants, very much like a_0
- derive from a two or three parameter universal potential
- have a simple chemical meaning (bonding model)
- reproduce correctly the first order spectroscopic constants (i.e. distinctively better than the results presented in Figure 2a and 2b using the Morse potential) and
- be situated between a_0 and D_e in order that the non-crossing rule can interfere to obtain the correct dissociation limit D_e . $D_x - D_e$ would then determine the critical distance.

We realize that skipping condition (ii) opens the way for other potentials with possibly universal characteristics.^[15] However, using a priori another dissociation limit to account for the observed PE curves, also a priori introduces an apparent error: this should constantly be kept in mind when comparing the performances of different potentials and asymptotes.

5.3.4 Scaling F and G by Ionic Sutherland Parameters

In principle, one could imagine various potentials with alternative asymptotes. We suggested that the ionic dissociation limit (and an ionic potential) is a good alternative,^[6] as it is almost as good a *natural* dissociation limit as the atomic one and, it is usually situated between a_0 and D_e . The alternative (AIM-) asymptote of Von Szentpaly^[15] seems to meet these constraints too, although his potential is not that transparent as an ionic one, it is not a reduced potential and the bonding model it relies upon is not that simple either (AIM-approach). A fairly good reason for choosing an ionic asymptote is that most of the aberrations showing in $F(\Delta)$ - and $G(\Delta)$ plots, when a covalent Δ is used (see Figure 2a–b), disappear, *in agreement with experiment*, when the covalent bond energy is replaced by the ionic bond energy *for both ionic and non-ionic molecules*.^{[6][7]} But, in general, two kinds of ionic asymptotes can be distinguished, depending on their D_e dependency.

5.3.4.1 Ionic Sutherland Parameter Depending on D_e

Only for dissociation in $A^+ + B^-$, a good approximation for the ionic Sutherland parameter is

$$\Delta_{\text{ion}} = 1/2 k_e R_e^2 / D_{\text{ion}} = a_0 / D_{\text{ion}} \quad (5a)$$

where

$$D_{\text{ion}} = \text{IE}_B - \text{EA}_A + D_e \quad (5b)$$

in which IE_X is the ionization energy and EA_X the electron affinity. However, this is a poor approximation for the ionic

asymptote of bonds with intermediate polarity. In addition, it will always depend upon D_e (for a general D_{ion} , valid for all types of bonds, see below).

5.3.4.2 Ionic Sutherland Parameter not depending on D_e

For ionic molecules, with a spectroscopic behavior rationalized by ionic functions, Varshni and Shukla^[4] already suggested another scaling parameter t , defined as

$$t = 2 + k_e R_e^3 / e^2 \quad (6)$$

independent of D_e and which relies upon an eigenvalue

$$D_x = e^2 / R_e \quad (7a)$$

corresponding with a different ionic (Coulomb) Sutherland parameter

$$\Delta'_{\text{ion}} = 1/2 k_e R_e^2 / D'_{\text{ion}} = a_0 / e^2 / R_e \quad (7b)$$

This is the most natural ionic asymptote imaginable in chemistry (Coulomb attraction between two point charges) and it is exactly the asymptote generated by a Kratzer potential. This asymptote can, when generally valid, be extended to all types of bonds without exception (for which R_e is known) and can even be applied to bonds for which D_e is not known, which is the case for many of the 400 bonds, inventoried in the present study.

5.3.5 Results with Ionic Sutherland Parameters – Discussion

For 40 bonds, the constants of non-ionic (i.e. covalent or homonuclear) molecules can be brought in line with ionic bonds just using an ionic Sutherland parameter.^[6] In addition, the RKR curves are correctly reproduced for different kinds of bonds.^[6] Not only $F(\Delta_{\text{ion}})$ and $G(\Delta_{\text{ion}})$ plots but also $F(t)$ and $G(t)$ plots show very smooth relations, not too far away from the ones theoretically expected by ionic potentials.^[6] Figure 2c illustrates these earlier findings on a larger scale for 91 single bonds, whereby experimental F values are plotted against the *square root* of the ionic Coulomb Sutherland parameter, simply related to the Varshni–Shukla parameter t :

$$\Delta'_{\text{ion}} = a_0 / e^2 / R_e = (1/2) k_e R_e^3 / e^2 = t/2 - 1 \quad (8)$$

We cannot but conclude from Figure 2c, in which no *gap* appears at all, that our suggestion to change the variable in the Dunham expansion and to use the alternative asymptote generated for scaling turns out to be very satisfactory. The slope of the trend line is almost *unity*, the intercept is almost *zero* and most data-points are on or very close to the empirical fit. The goodness of fit is over 0.9, including the data point for F_2 , which is the most notable exception. This is also an exception in the Von Szentpaly scheme^[15] and in many other instances.

In comparison with Figure 2a, Figure 2c represents a significant improvement, both practically and theoretically. We are now justified to elaborate the theoretical predictions of ionic potentials and to see whether or not they can be considered as universal (low parameter) potentials.

6. Universal Two-Parameter Functions: Theoretical Requirements

6.1 Ionic Potentials

Born,^[26] Pauling,^[27] and Mulliken^[28] all had a special interest for ionic potentials, which remain an important part of the chemical heritage (see Varshni and Shukla's review^[4] for alkali-halides, dissociating nearly into ions, with $D_e \approx D_{\text{ion}}$). The choice of empirical ionic potentials is very large^[4] and it is impossible to give a full overview here. However, since all ionic potentials are similar, we give two functions, bearing a direct relationship with Coulomb's law.

6.1.1 The Born–Landé Potential^[25]

$$U(R) = -e^2/R + B/R^n \quad (9)$$

is one of the oldest ionic potentials and it is a simplified version of the general Mecke^[29]–Sutherland^[11] function, used by Grüneisen^[30] and Mie^[31] in solid state physics. The potential was discussed by Varshni and Shukla.^[4] Their results for F and G in function of Δ are given in Table 1 below. Its asymptote equals

$$D_x = e^2(1 - 1/n)/R_e \quad (10)$$

and is, in general, larger than D_e . Values for n are obtained using ionization energies, electron affinities and D_e , which is always needed. In general $n \approx 9$, but $n = 2$ is a special case.

6.1.2 The Kratzer^[25]–Fues^[32] Potential

With $n = 2$ in (9), a Kratzer-type potential is generated, of the general form

$$U(R) = -2Ae^2/R + B/R^2 \quad (11)$$

which is a very attractive potential^[6,7,33,34]. This Coulomb function also generates a simple asymptote, comparable in magnitude with (10), and equal to

$$D_x = Ae^2/R_e \quad (12).$$

The Kratzer variable

$$\lambda = (R_e - R)/R \quad (13)$$

behaves almost exactly as the Dunham variable ρ around R_e (see above). With $A = 1$, this is even a *one parameter potential*.

In reduced form, the potential can be *forced* towards the atomic dissociation limit at infinite separation instead of to its natural asymptote (12), leading to

$$U(R) = D_e(1 - R_e/R)^2 \quad (14)$$

and then becomes a *two parameter potential*. Since we proposed the variable (13) to replace Dunham's ρ , an expansion of (14) in terms of ρ generates (ideal) ionic Dunham coefficients^[7]:

$$a_n = (-1)^n (n + 1) \quad (15)$$

Even these simple values are of the correct order of magnitude in a number of cases. With a deviation of $\pm 25\%$, these *mathematical* coefficients are obeyed by about 1/5 of 381 bonds:

- for $-a_1 = 2 \pm 0.50$: 108 bonds
- for $a_2 = 3 \pm 0.75$: 76 bonds.

In his analysis of the Kratzer potential, Varshni^[3] argued that this *two parameter potential* always gives $\Delta = 1$ (see Table 1), a value reserved exclusively for $D_x = a_0$. He remarked that this Δ value ($= 1$) did not occur in practice with a_0/D_e values and he had to reject the potential. In our set of over 300 bonds, we found 2.040 as the lowest value for the *covalent* Sutherland parameter (for T_2^+). Applying constraint (ii), Varshni could not try a different asymptote, although for ionic asymptotes, the situation $\Delta_{\text{ion}} < 1$ also occurs. Instead, he introduced a generalization, expected to yield better results, when coupled to D_e (see next section).

Although they did not mention Kratzer's work, Simons, Parr, and Finlan^[24] also attempted to remedy the convergence problem of the Dunham series, i.e. its wrong behavior at $R = \infty$, by using the Kratzer variable λ , leading to a function known as the SPF potential. Despite the advantages the SPF potential certainly has, we showed^[7] a long time ago that this can never be an appropriate solution. In the SPF theory λ remains coupled with (if not to say forced to) the atomic dissociation energy, which is not its natural eigenvalue.

6.1.3 Generalized Kratzer Potentials

The Varshni-V potential^[3]

$$U(R) = D_e[1 - (R_e/R)^m]^2 \quad (16)$$

is a straightforward generalization of the Kratzer potential (14), although the asymptote should be e^2/R_e , and not D_e . The corresponding *reduced* generalized function is

$$U(R)/D_e = [1 - (R_e/R)^m]^2 = (1 - r^{-m})^2 \quad (17)$$

with $R = rR_e$, r being a number, obeying $0 \leq r \leq \infty$. This potential was applied to a variety of bonds with satisfactory results, only after replacing D_e with D_{ion} .^{[6][7]} This generalization leads to the F and G expressions, collected in Table 1, where the potential is denoted by *Kratzer I-Varshni V*. Reminding Figure 2c, the identity $F = m = \Delta^{1/2}$ is intriguing. We will test here

$$U(R) = Ae^2/R_e[1 - (R_e/R)^m]^2 \quad (18)$$

With $A = 1$, this is a *two parameter* (R_e and m) *ionic potential*: just two parameters, R_e and k_e , suffice to reach a first order solution for the spectroscopic constants. The third parameter, available for further fitting, is A in Equation (18), as the only practical further scaling element is the Coulomb interaction. Here, parameterization in terms of the Calder–Ruedenberg idea of a Column classification (ionicity, charge-effects, ...) can logically be considered (see Figure 1). Only if the results obtained with $A = 1$ are acceptable for bonds with one or two monovalent atoms, we can allow other A values (for instance for multiple bonds). In cases where $A \neq 1$, we deal with a *three-parameter potential*.

Other generalizations of the Kratzer potential are possible^[7]: a ratio $(R_e + a)/(R + a)$ leads to

$$\begin{aligned} U(R) &= D_x [1 - (R_e + a)/(R + a)]^2 \\ &= D_x (1 - R_e/R)^2 [1/(1 + a/R_e)]^2 \end{aligned} \quad (19)$$

in which the original Kratzer potential is multiplied by the square of a normalizing or scaling factor $y = 1/(1 + a/R_e)$. Expanding this alternative generalized Kratzer function in ρ , we get $F = 2\Delta^{1/2} - 1$ (see Table 1) as the Dunham coefficients will now be given by^[7]

$$a_n = (-\Delta^{1/2})^n (n + 1) \quad (20)$$

These are scaled coefficients with respect to the ideal ionic ones given in Equation (15), where $\Delta^{1/2} = 1$. Results are collected in Table 1 under the potential *Kratzer II*. If D_x is an ionic dissociation limit computed from atomic data or computed directly from R_e , *ionic functions remain two parameter potentials*.

6.2 Ionic Dissociation Energy and the Ground State of Molecules

6.2.1 The Born–Landé Asymptote

To avoid the cumbersome procedure to obtain the n values needed for the Born–Landé asymptote (10), we want to replace it with a simpler variant, also independent of D_e .

Normally, ionic bond energies (asymptotes) are either given by $IE_A - EA_B + D_e$ for dissociation into A^+ and B^- or $IE_B - EA_A + D_e$ for dissociation into A^- and B^+ and, in both cases, D_e is needed. For bonds of intermediate polarity, the situation is less clear. If B has the higher electronegativity and *if both ionic forms are present in the ground state in a ratio b^2/a^2 with $a^2 + b^2 = 1$* , this virtual ionic dissociation energy would not be available experimentally. We can try to calculate it by putting

$$\begin{aligned} e^2(1 - 1/n)/R_e &= a^2[(IE_B - EA_A) + D_e] + b^2[(IE_A - EA_B) + D_e] \\ &= [IE_A + a^2(IE_B - IE_A)] - (a^2EA_A + b^2EA_B) + D_e \end{aligned} \quad (21a)$$

$$\approx IE_A + a^2(IE_B - IE_A) \quad (21b)$$

In going from Equation (21a) to (21b), we used the intermediate result,^[34] that, in first approximation,

$$D_e = a^2 EA_A + b^2 EA_B \quad (22)$$

and this might remove D_e from the ionic bond energies in a systematic way.

With the definition of the bond polarity $I = b^2 - a^2$, this ionic asymptote will further reduce to

$$e^2(1 - 1/n)/R_e \approx IE_A + (1 - I)(IE_B - IE_A)/2 \quad (23)$$

$$\approx 1/2(IE_A + IE_B)(1 - I^2) \quad (24)$$

if $I = (IE_B - IE_A)/(IE_A + IE_B)$ is used as a first order approximation for the bond polarity I .

Strictly spoken, I should depend on electronegativities, according to Wilmschurst.^[35] Using IE_X as an approximation for either the Pauling^[36] electronegativity χ_P or Mulliken's^[37] $\chi_M = (IE_X + EA_X)/2$ is acceptable, especially if Mulliken's definition is taken as a guideline (in general $IE_X \gg EA_X$). The only theoretical advantage of these deductions is a simplification of the ionic bond energy (21), which can now be computed from available atomic quantities (ground state ionization energies of atoms), as intended. Using Pauling χ_P values would not alter much to the result for the asymptote (except in a few cases).

The asymptote for a virtual dissociation in $a^2(A^- + B^+) + b^2(A^+ + B^-)$ gives an idea of the bonding situation at R_e , since the bonding partners, isolated at $R = \infty$, are frozen in the same (*charged*) states they had at the equilibrium distance (IIM method).

Developing (23) further shows that

$$e^2(1 - 1/n)/R_e \approx 2 IE_A IE_B / (IE_A + IE_B) \quad (25)$$

For homonuclear bonds XX, we get

$$e^2(1 - 1/n)/R_e \approx (IE_X - EA_X) + D_e \approx IE_X \quad (26)$$

if the difference between EA_X and D_e is not too large.

Using this approximation would again lead to a *two-parameter* potential, at least for bonds between monovalent atoms, whereby just k_e and R_e will be needed to compute F and G . Additional refinements are possible using valence state ionization energies instead of ground state values, similar an approach as suggested by Von Szentpaly in his AIM approximation.^[15]

Rewriting Equation (25) in function of effective charges q_X and covalent radii r_X of atoms X and using $IE_X = q_X e^2/2r_X$, where q_X and r_X are respectively the effective nuclear charge (for the valence electron) and the covalent radius of atom X, we obtain

$$e^2(1 - 1/n)/R_e = e^2(1 - I^2)(q_A r_B + q_B r_A)/r_A r_B.$$

If both q_A and q_B are not too different from 1, a standard relation results for the bond length

$$R_e \approx r_A + r_B$$

since the two polarity terms will cancel in first approximation. This brings ionic bond energies in line with the Kratzer asymptote, as intended by eliminating D_e in the Born–Landé asymptote.

6.2.2 The Kratzer Asymptote

Whether or not the Kratzer asymptote e^2/R_e is (or must be) the same as the Born–Landé asymptote is not clear. The predictions of these two ionic potentials will therefore be tested as such. We notice the dependence of the theoretical ionic bond energies upon $(1 - I^2)$ in Equation (23), which also suggests an alternative Kratzer I asymptote equal to

$$D_x = e^2(1 - I^2)/R_e \quad (27)$$

This corresponds with A in (18) equal to $(1 - I^2)$, a correction for charge transfer in the bond. If valid, this means that for two interacting charges at equilibrium the following Equation applies

$$A = q_A q_B = A'(1 - I)(1 + I) = A'(1 - I^2) \quad (28)$$

if $q_X \approx 1 \pm I$, a strange formula for ionic bonds anyhow ($I = 1$ would mean $A = 0$), to be tested below with the spectroscopic constants. $A' = 1$ in Equation (28) would still give rise to two parameter Kratzer potentials, since I can be calculated from atomic quantities. It must be noticed that A will not only be determined by the atom's partial *charge* ($\pm I$) but also by its *valence* (which is a Column classification effect, as noticed by Calder and Ruedenberg^[5]).

6.3 Relations Between the First-Order Parameters F and G and the Scaling Factor Δ for Some Standard Potentials

According to Varshni's procedure,^[3] the higher derivatives of potentials, scaled by the second, result in relations between F and G and the Sutherland parameter Δ , shown in Table 1. Most potentials can be considered as two or three parameter functions (see above), only Morse's function is always a *three-parameter* potential. First order-zeroth order relations like $F(\Delta)$ allow a computation of D_x values, the intermediate asymptotes, directly from the spectroscopic constants for each of the potentials mentioned in Table 1.

For the same Δ values, large differences are expected for $F(\Delta)$ and $G(\Delta)$. Leaving out the Kratzer potential, the following F values are respectively obtained for $\Delta = 9$: 6.33, 3.00, 5.00, and 2.00 (difference > 300%). Differences (in%) for $\Delta = 1$ would be larger, as the respective F values are equal to 1.00, 1.00, 1.00, and 0.

Translating this into D_x values gives for $F = 2$ values ranging from $a_0/2.666$ to $a_0/0.41$, a ratio of 1/6.5, which must be clearly visible. Since, in theory, there are no differences between the Δ 's in Table 1 (in a standard theory, they all equal the *covalent* Sutherland parameter), this would lead to conflicts, when the relative merits of potentials are to be compared, and universal scaling would become practically impossible (see Figure 2).

The resulting $G(F)$ relations and the G/F ratios, are similar, as they all start with a scaling factor $(1 + F)^2$. This factor relates to $a_1 = -(1 + F)$. Comparing the potentials

Table 1. $F(\Delta)$, $G(\Delta)$, and $G(F)$ relations according to some potentials

Potential	$F =$	$G =$	$G(F)$	G/F value	
Born–Landé	$2\Delta/3 + 1/3$	$(8\Delta^2 + 38\Delta + 26)/3$	$3 + 15F + 6F^2$ $= 6(1 + F)^2 + 3(F - 1)$	for $F = 1$ 24	$F = 3$ 34
Kratzer	1	24	24	24	24
Kratzer I (= Varshni V)	$\Delta^{1/2}$	$8\Delta + 12\Delta^{1/2} + 4$	$(= 6(1 + F)^2)$ $4 + 12F + 8F^2$	28	39
Kratzer II	$2\Delta^{1/2} - 1$	24Δ	$= 8(1 + F)^2 - 4(1 + F)$ $6 + 12F + 6F^2$	24	32
Morse	$\Delta^{1/2} - 1$	8Δ	$= 6(1 + F)^2$ $8 + 16F + 8F^2$ $= 8(1 + F)^2$	32	43

shows that, theoretically, Morse's potential gives the highest G values, followed by Kratzer I, Born–Landé, and Kratzer II in that order.

6.4 The G/F Ratio

Table 1 shows that theoretical G/F ratios obey equations of the general form

$$G/F = aF + b + c/F \dots \quad (29)$$

where a , b , and c are constants and where the exponent of F [equal to 1 in Equation (29)] depends on the potential. Predictions about G/F values are roughly comparable with observed values.

In terms of the constants and according to Varshni's definition,^[3] the G/F ratio obeys

$$\begin{aligned} G/F &\approx (\omega_e x_e / \omega_e) (B_e / a_e) \\ &\approx (B_e / \omega_e) (\omega_e x_e / a_e) \\ &\approx \omega_e x_e B_e / a_e \omega_e \end{aligned} \quad (30)$$

independent of Δ and in which all lower order constants are pair-wise coupled in a symmetrical (vibrational/rotational or first order/zeroth order) or in an anti-symmetrical way. The normalizing factor for G , to distinguish between potentials, should rather be a_1^2 or $(1+F)^2$ (as in the Graves–Parr scheme^[2]), but this would destroy part of the relation of the G/F ratio with the four constants in Equation (30). The G/F ratio plays an important role in other scaling schemes, although this is not always apparent in the original publications.

6.4.1 The G/F Ratio and the Calder–Ruedenberg Constant C

In the first large-scale analysis on constants of 160 diatomics, Calder and Ruedenberg^[5] concluded 30 years ago that the G/F ratio is a constant C and that it is equal to

$$C = 4(1+a_1)/(a_2 - 5a_1^2/4) \approx 1.39 (\pm 5\%) \quad (31)$$

The reported error of 5% for 160 bonds sounds impressive. They did not mention, however, that this constant C bears an intimate numerical relation with the G/F ratio:

$$G/F = 48/C \quad (32)$$

This follows from the relations between F and G and the lower order Dunham coefficients:

$$a_1 = -(1 + F) \quad (33a)$$

$$a_2 = (5/4) a_1^2 - G/12 \quad (33b)$$

since substituting (33a) and (33b) in (31) immediately gives (32). Very unfortunately, Calder and Ruedenberg did not at all discuss *potentials*: they restricted their analysis to the constants.

Translating their analysis to potentials and predicted G/F values [Table 1 and Equation (29)] leads to a contradiction: C can never be a constant as it will always depend upon F in a particular way for each of the potentials in Table 1 (see also Varshni^[3] for other examples).

In the case of the Kratzer II potential, $C = 8F/(1 + F)^2$ leads to $C = 0$ for $F = 0$, with a maximum of 2 for $F = 1$ and then gradually decreasing with increasing F to 1.33 for $F = 4$. These predictions are roughly in line with observation, even Calder and Ruedenberg's: C values in general decrease with increasing F (or $-a_1$) values. Even the reputed Morse potential gives a similar result for C . With the ideal ionic coefficients (15), the constant C is equal to 2, of the correct order of magnitude.^[7]

We showed some time ago how the difference between the asymptote D_x and the atomic asymptote D_e can influence quantitatively C values,^[7] which, if true, might also point towards an external influence on G/F values (see further below).

Calder–Ruedenberg's idea of a constant C arose from classifying molecules in function of the position of the atoms in the columns of the Periodic Table (which might be a very rough intuitive measure for *valence* and for *bond ionicity* too, see above). This classification is justified by relations found between constants, whereby a clustering was observed for bonds between atoms in the same Columns of the Table (as illustrated in Figure 1b). Graves and Parr^[2] also used the Column classification. However, these authors concluded that it did not help *significantly* to reveal scaling trends, in clear contradiction with the Calder–Ruedenberg analysis, its claimed accuracy and its conclusion.

The Graves–Parr conclusion is in line with our discussion about scaling given above (see Figure 1a–b) and we

will discuss the matter more fully below in another context. Despite this negative conclusion of Graves and Parr, the idea for a possible grouping of molecules in the spirit of Calder and Ruedenberg remains important in the context of Coulomb attraction

$$q_A q_B e^2 / R \quad (34)$$

We refer to the discussion of A values in Equation (28), in terms of *charge* and *valence* effects. Strictly spoken, the Calder–Ruedenberg classification invokes an additional (hidden) parameter, not yet quantified. In line with the remarks by Graves and Parr, we will show that several of the Calder–Ruedenberg groups overlap (see also Figure 1b).

6.4.2 The G/F Ratio and the Graves–Parr Scaling System

In addition, in the Graves–Parr scaling system, the G/F ratio plays a dominant role, although this is not apparent in their paper.^[2] They showed that the Dunham coefficients a_1 and a_2 should both be scaled by the *covalent* Sutherland parameter. With perfect scaling, the ratio of a_1^2/Δ and a_2/Δ should theoretically be a constant. However, statistical effects, not mentioned by Graves and Parr, will also increase the goodness of fit with respect to the unscaled coefficients. Table 2 gives some results.

Table 2. Graves–Parr scaling procedure

Potential	$a_1^2 =$	$a_2 =$	$a_1^2/a_2 =$
Kratzer	4	3	$4/3 = 1.333$
Kratzer I – Varshni V	$(1 + \Delta^{1/2})^2$	$7/12(1 + \Delta^{1/2})^2 + (1/3)(1 + \Delta^{1/2})$	$1.714/(1 + 4/[7(1 + \Delta^{1/2})])$
Kratzer II	4Δ	3Δ	$4/3 = 1.333$
Morse	Δ	$(7/12)\Delta$	$12/7 = 1.714$

The relations between the Dunham coefficients and the Varshni parameters F and G in Equation (33) show that a_1^2/a_2 is also determined by the G/F ratio. Whereas 3 potentials lead to a constant, only the Kratzer–I–Varshni–V function predicts that a_1^2/a_2 should be a function of $\Delta^{1/2}$ (or of F).

6.4.3 The G/F Ratio: Chaotic/Fractal Behavior

Freeman, March and Von Szentpaly^[16] argued that an empirical power $G(F)$ relation exists

$$G = 27.4F^{4/3} \quad (35)$$

This, in their opinion, suggests chaotic/fractal behavior. Equation (35) leads to the ratio

$$G/F = 27.4F^{1/3} \quad (36)$$

resulting in the values 27 and 40 for F equal to 1 and 3, comparable with those in Table 1.

If this relation were reliable, this would probably complicate the search for a universal potential.

7. Universal Two-Parameter Functions: Theory versus Experiment

7.1 Lower-Order Constants

The spectroscopic constants ω_e , $\omega_e x_e$, B_e , and α_e exhibit intriguing relations, some of which were discussed already above and also by Calder and Ruedenberg^[5] in order to justify the Column classification and by Herschbach and Laurie^[19] for the Row classification. These will not be repeated here, although we discuss 100 bonds containing H, of which only 10 were included in the Calder–Ruedenberg analysis (one relation was extended to H bonds in Figure 1a and 1b).

We first present the results for the last identity in Equation (30) for 381 diatomic molecules in Figure 3. The empirical *power* relation (logarithmic scale), valid for differences of the order of 10^7 in the two axes, combined with a high R^2 value, is not significantly better than the empirical *linear* relation. Since these also determine the G/F ratio, chaotic/fractal behavior^[16] may be put in doubt. The accuracy for the computed product of a pair of two constants is 10% for 381 bonds, which illustrates the overall quality of the relations between the constants. Various other relations are found. In some cases, an empirical power relation gives a goodness of fit of (over) 0.9, as can be seen from the results in Table 3. It is not always clear, however, whether or not this is due to large-scale differences or to a basic relation between the constants. We believe this is a matter of further research.

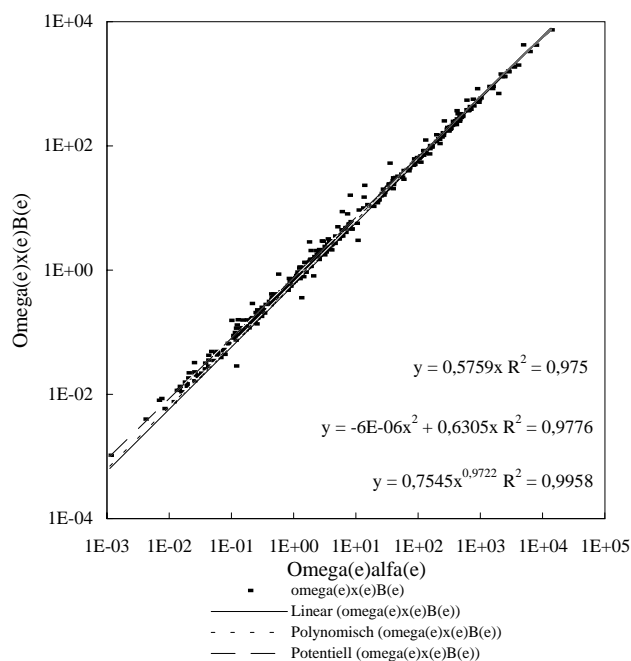


Figure 3. G/F : $\omega_e x_e B_e$ versus $\omega_e \alpha_e$ for 380 bonds

Table 3. Empirical power relations between observed spectroscopic constants ω_e , $\omega_e x_e$, B_e and α_e and equivalents for $14.4/R_e$ and a_0 (cm^{-1}) for 381 bonds and D_e (eV) for 300 bonds

$Y(X)$	Empirical $Y(X)$ relation	R^2	Remark
$\omega_e(\alpha_e)$	$3363.4X^{0.2996}$	0.7315	
$\omega_e(\omega_e x_e)$	$304.6X^{0.5386}$	0.8086	
$\omega_e(B_e)$	$894.48X^{0.4546}$	0.8336	
$\omega_e x_e(B_e)$	$7.2793X^{0.8044}$	0.9368	important for G , Equation (4)
$\omega_e x_e(\alpha_e)$	$92.138X^{0.5691}$	0.9466	corresponding with a $G(F)$ relation
$B_e(\alpha_e)$	$22.111X^{0.6956}$	0.9769	best fit, important for F , Equation (3)
$\omega_e(14.4/R_e)$	$3.6185X^{2.5694}$	0.8456	
$\omega_e(D_e)$	$391.38X^{0.5584}$	0.2166	for 300 bonds with D_e known
$\omega_e(a_0)$	$41.183X^{0.2372}$	0.0393	

For 381 bonds, the 6 relations between the constants in the upper part of Table 3 are quite reliable, the best being the 6th $B_e(\alpha_e)$ in terms of R^2 . This empirical power relation reproduces B_e values from α_e with an average absolute deviation of 10% for most bonds. The 5th corresponds with a $G(F)$ relation (see above). Two other relations with a relative good fit are important for F and G .

The second part of Table 3 gives a confrontation of 3 asymptotes as to their possible relationships with the harmonic frequency, for which the R^2 values are much higher than for the remaining three spectroscopic constants (not shown). For the asymptotes D_e and a_0 , there is no significant global relation. The situation is different for the ionic asymptote. However, if the asymptotes (x values) are corrected for reduced masses, the goodness of fit is drastically improved for all asymptotes (for the Kratzer asymptote, even the identity results in the case of B_e). Therefore, the groupings observed in Figure 1a and 1b originate for the larger part from the reduced masses. This is most apparent for H-containing bonds, which seem to form a different spectroscopic group (see Figure 1 and next sections).

7.2 Derived Constants (a_0 , k_e , Δ , F , G)

We first confront the asymptotes with the harmonic frequency according to the Column classification (see also Table 3). As remarked by Calder and Ruedenberg,^[5] the intuitively sound relation between the two most important constants of a bond, i.e. a_0 and ω_e , can be visualized in the corresponding plot (Figure 4a). Although a_0 depends on the square of ω_e by definition, no straight general relation is observed, except for some classes of bonds. In agreement with the situation in Figure 1a–b, also here we find regularities (Row- or Column classifications). Figure 4a also shows *why* Calder and Ruedenberg excluded most H-containing bonds from their analysis: these distinctly form a different spectroscopic class and the dividing line between H-containing molecules and the other is clearly visible. This line would be situated exactly where a breaking of the symmetry occurs between atom mass M and atom number Z ,

i.e. at $Z = 1$. Merely using Hooke's law to account for the constants (as in Dunham's oscillator model, where forces depend on masses) is not uniformly applicable throughout the Periodic Table.

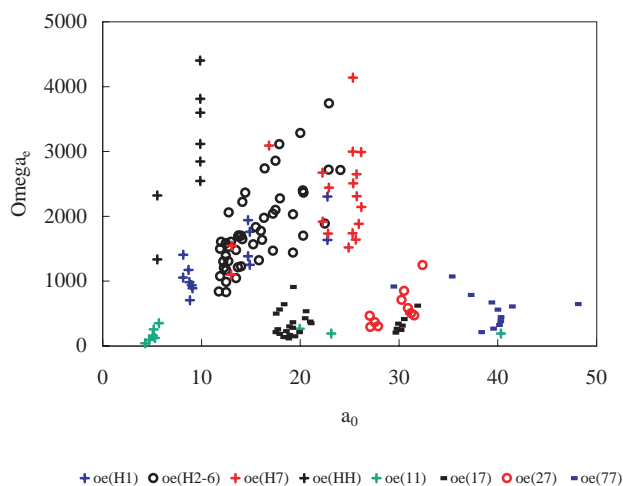
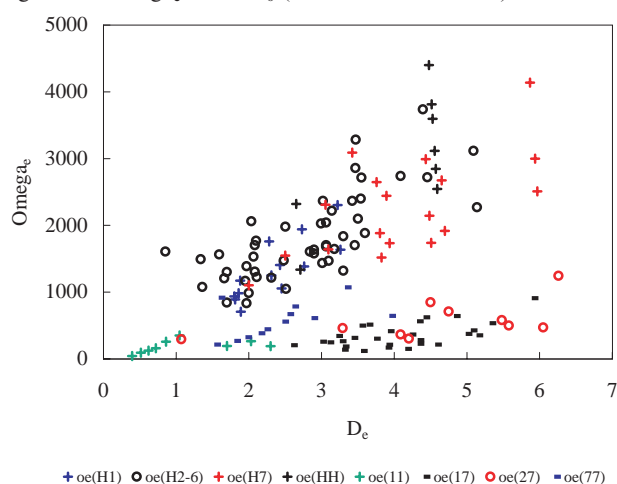
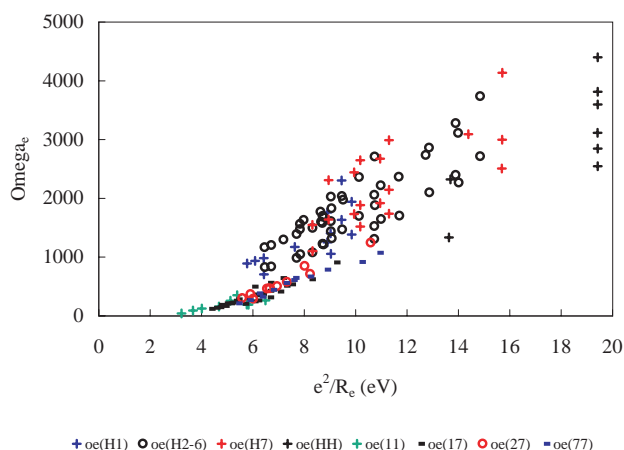
Next, substituting a_0 with D_e (Figure 4b) does not improve the picture at all and no new or better global relationship emerges, on the contrary (in agreement with the results in Table 3). The only classes of bonds for which regularities appear (Column-classes 11, 77, and 27) are also grouped or equally regular in Figure 4a. For other groups, the regularities in Figure 4a have disappeared. This seems to justify our suggestion that D_e , the atomic dissociation limit, is only reached in a number of cases, after other effects have been operating between R_e and ∞ . Therefore, it seems fair to exclude constraint (ii) in a search for a universal potential (see also Table 3).

Thirdly, substituting a_0 with the ionic dissociation energy (calculated from ionization energies, the Kratzer II asymptote) leads to a better picture (not shown) but which is intermediate with that obtained when one replaces a_0 with the Kratzer I asymptote. Figure 4c gives the plot for e^2/R_e . A similar plot has already been given in Figure 1, since $(B_e)^{1/2}$ can be used as a substitute for e^2/R_e in the x -axis. Figure 1 being an ω_e ($1/\mu R^2$) plot, it is readily concluded that this leads to a completely different picture than the one having a_0 in the x -axis (Figure 4a) both for the H-containing bonds and for other bonds. In fact, and contrary to Figure 4b for D_e , and apart from the scaling and classification effects already discussed above, Figure 4c also shows how well the harmonic frequencies of bonds are correlated with $1/R_e$. This dependence is characteristic for ionic potentials and we remind thereby that multiple bonds were not even excluded from these Figures. As well as the results in Table 3, this strengthens our ideas about the correct variable for the oscillator presentation. Indeed, Figure 4c gives large-scale evidence for the intuitive idea that an ionic Coulomb law seems to govern bond mechanics and that charges and valences are important to account for trends in the harmonic frequencies of bonds.

The details of clustering or classification in Figure 1a and 1b were discussed above. However, we must now remark that, in Figure 1b, the parallel lines are more close to each other and even extend linearly into the H group (points on the right side in Figure 1b). The number of lines that must be drawn in Figure 1b to encompass all data points seems less than in Figure 1a.

In terms of an additional parameter for a potential, it seems that a few values for A in Equation (28) would be sufficient to unify the complete picture in Figure 1b.

Experiment clearly shows, through Figure 4c, that the ionic dissociation limit can indeed be a serious candidate for explaining the relations between the spectroscopic constants. This asymptote seems very suited also for scaling a_0 , as it correlates extremely well with the two zeroth order constants, which completely determine a_0 . These are exactly some of the constraints for the alternative asymptote, given above. The transformation of the Dunham variable into the Kratzer variable for which we gave theoretical arguments

Figure 4a. Ω_e versus a_0 (Column-classification)Figure 4b. Ω_e versus D_e (Column-classification)Figure 4c. Ω_e versus e^2/R_e (Column-classification)

above, seems to be very effective indeed and is confirmed by experiment (see Figure 4c and Table 3).

7.3 Atomic Mass-Atomic Charge Symmetry Breaking

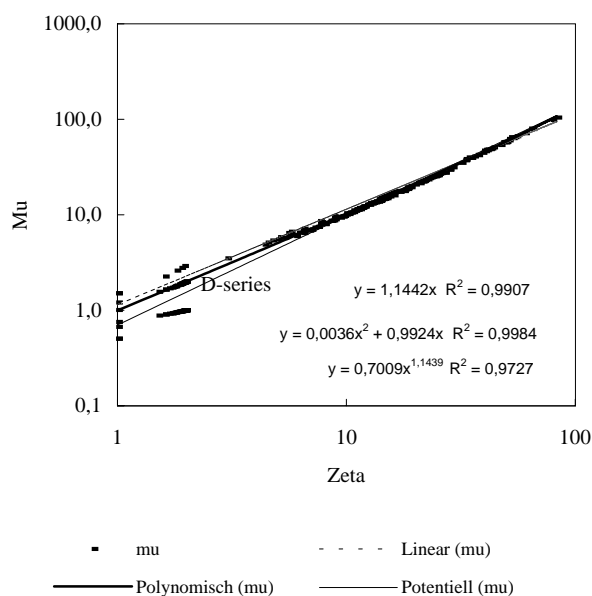
If we compare Figure 4c with the corresponding Figure 4a–b, we already notice a significant improvement in the

relation between the harmonic frequency and the asymptote. Since Figure 1a and Figure 1b are a justification for the two classification schemes (by Row or by Column), we now find a third effect operating in this correlation: symmetry breaking between atomic masses and atomic charges.

To illustrate this symmetry-breaking effect, we made a plot (Figure 5) of the reduced mass μ versus its equivalent ζ in terms of atom numbers Z , or

$$\zeta = 2Z_A Z_B / (Z_A + Z_B) \quad (37)$$

since, roughly, $M_X = 2Z_X$, especially in the lower part of the Periodic Table ($Z < 50$). Although a linear or a power fit gives R^2 values equal to almost unity, only a log-scale reveals the details of the symmetry-breaking effect at $Z = 1$ (see Figure 5). Only D-containing bonds follow the trend of the general relation. Reduced masses are determined by Rows and by Columns, as well as reduced atomic charges (atom numbers Z).

Figure 5. μ versus ζ for 300 bonds

In fact, most of the discontinuities between H- and non-H bonds in Figure 1a–b disappear if the square root of the harmonic frequency is plotted against an R value, that is corrected for a symmetry breaking effect at $Z = 1$, or

$$R_{\text{corr}} = R_e (\zeta/\mu)^{1/2} \quad (38)$$

The result is shown in Figure 6a which should be compared with Figure 4c (see above) to notice the global effect. The goodness of fit for a linear relation is 0.93, for a power fit it is 0.95 and for a quadratic one it is over 0.97. This is an improvement over the situation with the Dunham asymptote plotted against the harmonic frequency (Figure 4a) and may even question the validity of the classification schemes, discussed above, as all data-points seem to gather around a *single* line. For instance Row- or Column classifications are hardly visible (see Figure 6b for a log-log plot), and if persistent, hardly quantifiable. A comparison of Fig-

ure 6b with Figure 1 shows the scaling effects we were looking for.

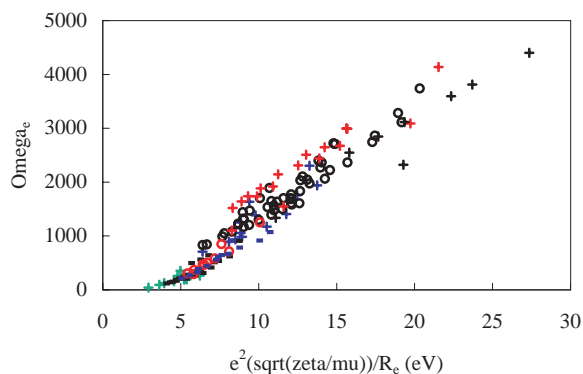


Figure 6a. Ω_{e} versus $e^2(\sqrt{\zeta/\mu})/R_{\text{e}}$ (Column-classification)

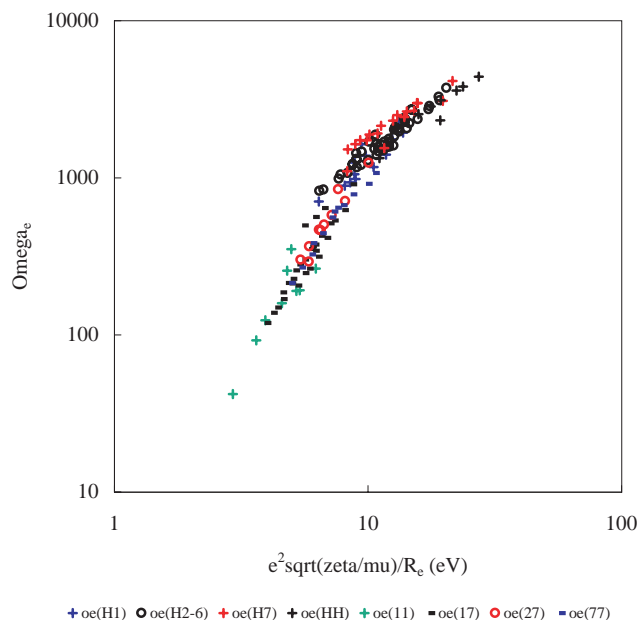


Figure 6b. Ω_{e} versus $e^2\sqrt{\zeta/\mu}/R_{\text{e}}$ (Column-classification) (log-scale)

These results are in agreement with classical dynamics (the dependence of the frequency on the ratio Z/M). This generalization of the ω_{e} ($1/R_{\text{e}}$) relation provides us with a possibility to achieve universal scaling in terms of charges and Coulomb-like potentials, reminding thereby the spectroscopic definition of a_0 , see Equation (2b).

7.4 Experimental and Theoretical $G(F)$ Relations

Unlike the $F(\Delta)$ - and $G(\Delta)$ relations (see Figure 2a and 2b), the $G(F)$ relation is completely determined by the spectroscopic constants. This relation represents a challenge for potentials and for scaling (see for instance the $\omega_{\text{e}}x_{\text{e}}$ (a_{e}) dependence in Table 3). We now confront the experimental $G(F)$ relation with the predictions of the potentials in Table 1.

Figure 7a presents the global view for the 381 diatomics with both G and F available. The best fit of a quadratic

relation nearly goes through the origin (intercept -1.38), but the coefficients of F are 7.4 for the quadratic and 21.8 for the linear term (see the Equations in Table 1). The power fit gives $28.974F^{1.2978}$, not too far away from the Freeman fit (see Equation 35). Both empirical relations have the same goodness of fit of $R^2 = 0.843$. We observe that the Morse function is closest to the empirical fit, followed by the Kratzer I potential. The goodness of fit is in agreement with that found for the $\omega_{\text{e}}x_{\text{e}}$ (a_{e}) relation in Table 3.

Nevertheless, there is a strong bias from exotic molecules (Van der Waals molecules, excited states, ...) with anomalous G/F values. Leaving out all excited states and extreme cases gives Figure 7b for some 300 bonds. The empirical quadratic equation is (only) slightly better than the power relation. This empirical quadratic relation gives G ($\approx \omega_{\text{e}}x_{\text{e}}$) from F ($\approx a_{\text{e}}$) within 9.8% of experiment, which is quite accurate given the number and the different kinds of molecules. The empirical fit lies between the Morse and Kratzer curves, but is closer to Morse's. The coefficients compare well with the theoretical ones given in Table 1.

At this stage (Figure 7a and 7b), the enlargement of the data-sample does not favor the conclusion of Freeman et al.^[16] about chaotic/fractal behavior, especially not in terms of the goodness of fit. Further material at high F values, where the empirical approaches diverge (Figure 7a), might be decisive in this respect, although this information will be hard to find.

We notice from Figure 7a and 7b that the Morse potential seems to validate Jhung's hypothesis^[9] and that the Kratzer I potential is low (see also our discussion of Table 1).

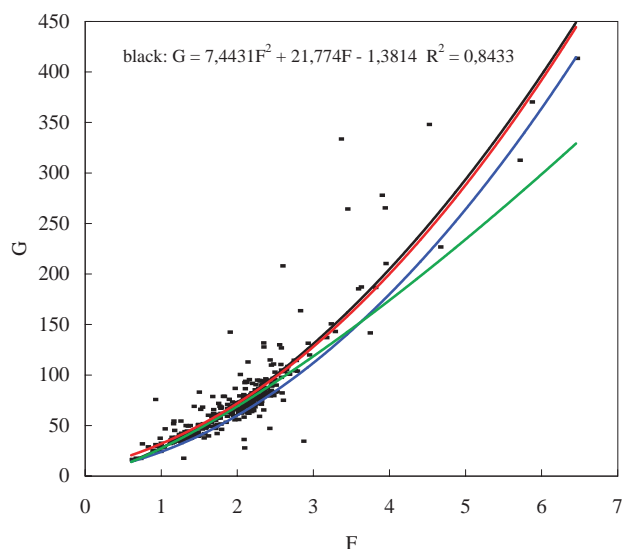
When the set is limited to 91 bonds between monovalent atoms (Figure 7c), different equations are generated. We now have $G = 9.55F^2 + 9.473F + 10.355$ with $R^2 = 0.9439$ and $G = 30.012F^{1.2162}$ with $R^2 = 0.9405$ (not shown), which are again close to the theoretical relations given in Table 1. Comparing the theoretical results of Table 1 with those of empirical quadratic fitting leads us to conclude that the Morse and the Kratzer I potential are the best choices in that order for reproducing the empirical $G(F)$ plot.

A different situation is found, when the theoretical predictions by the potentials are considered for the $G(\Delta)$ relation (see below). For the 91 bonds between monovalent atoms, the Morse results were already given above (Figure 2b), with a goodness of fit of only 0.5786 and a slope of 1.067 for an intercept of -3.57 in the case of a linear fit.

7.5 Predictions for First-Order Constants α_{e} and $\omega_{\text{e}}x_{\text{e}}$: Comparing the Performance of Kratzer and Morse Potentials

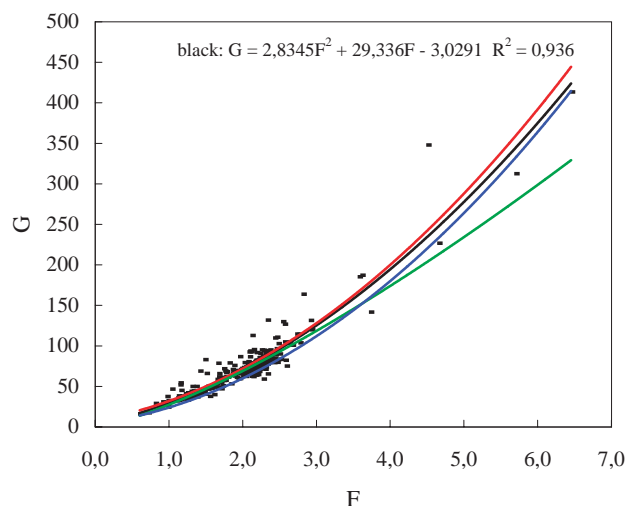
7.5.1 Ionic Sutherland Parameters for 91 Single Bonds and F

Figure 8a gives a plot of the three ionic Sutherland parameters versus F for 91 bonds between monovalent atoms. Even including F_2 (with $F = 2.667$), the goodness of fit for



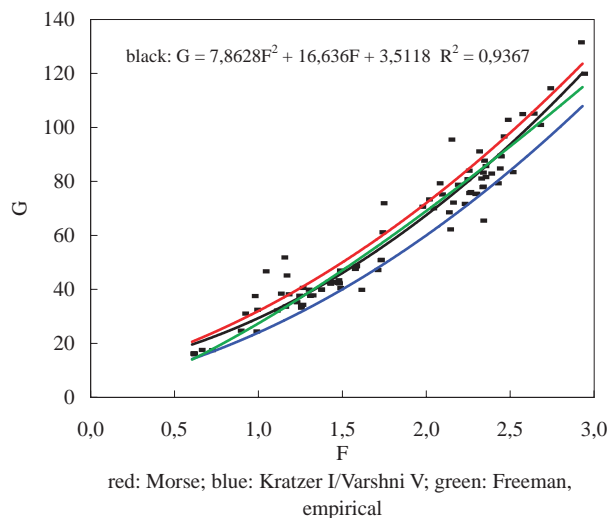
red: Morse; blue Kratzer I/Varshni V, green Freeman..., empirical

Figure 7a. Plot of G versus F for 381 bonds



red: Morse; blue: Kratzer I/Varshni V; green: Freeman, empirical

Figure 7b. G versus F for 300 bonds



red: Morse; blue: Kratzer I/Varshni V; green: Freeman, empirical

Figure 7c. G versus F for 91 single bonded diatomics

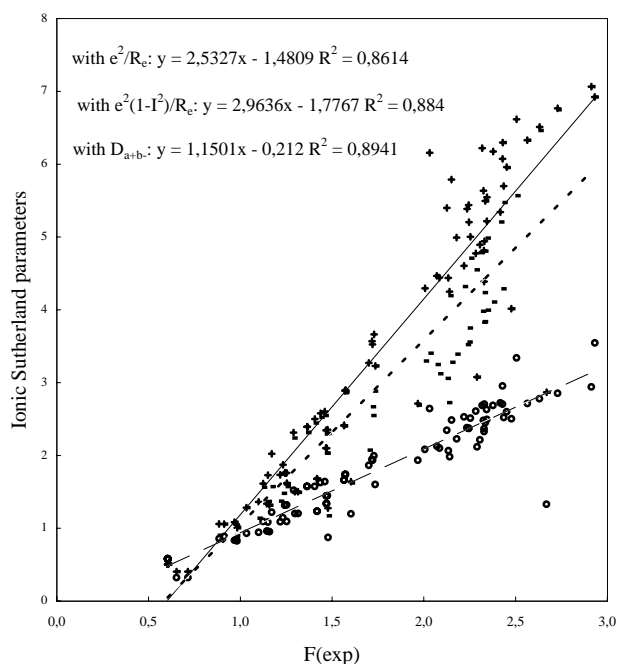


Figure 8a. Plot of 3 ionic Sutherland parameters versus F(exp) for 91 single bonded diatomics

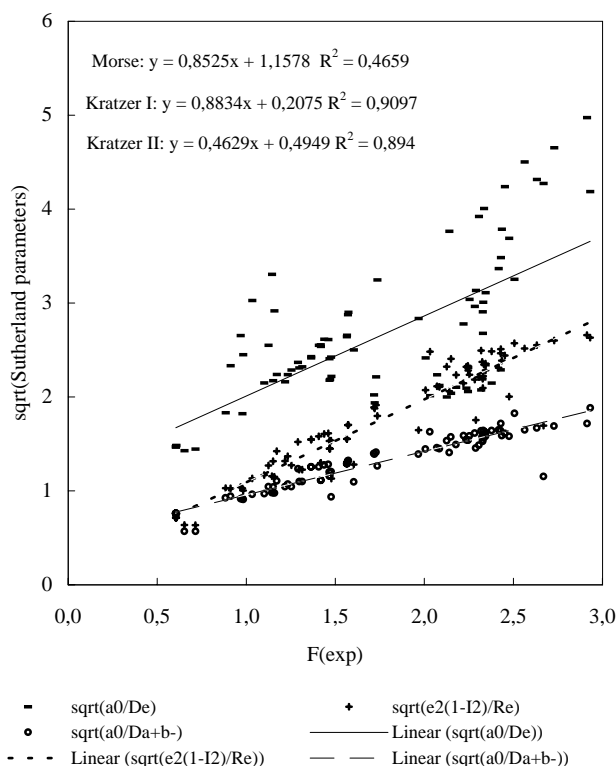


Figure 8b. Square root of different Sutherland parameters versus F for 91 single bonded diatomics

all ionic asymptotes is relatively high. The series, based upon D_{A+B-} , calculated from ionization potentials, has polarity effects $(1 - I^2)$ included automatically. The trends observed show that a quadratic dependence might be better (see the Graves–Parr suggestion and see Table 1).

Figure 8b represents the results with $\sqrt{\Delta}$ for the same 91 bonds but now the covalent Sutherland parameter is included for comparison (see also Figure 2). Despite the scale differences, it is readily concluded that *any ionic Sutherland parameter is superior to the covalent one*. Slopes and intercepts are as expected, even for the Morse relation. The covalent Sutherland parameter may be plausible for some (classes of) molecules. About 50 are situated near the theoretical line but 40 are completely out of range (another illustration of Varshni's earlier observation and of the spectroscopic gap, artificially created by the covalent Sutherland parameter, see above).

The predictions of a Kratzer potential are good. Empirical fitting through the origin yields the theoretically expected coefficient of nearly 1, with a goodness of fit almost identical to a linear fit, with a free intercept (not shown). The other series, based upon D_{A+B-} (also promoting the Born–Landé potential in Figure 8a) practically leads to a relation of the form

$$F = 2\Delta^{1/2} - 1 \text{ or } \Delta^{1/2} = F/2 + 1/2$$

(goodness of fit 0.89). This corresponds with the predictions of the *Kratzer II* potential.

Since the polarity I of the bond is computed from *atomic* quantities, Figure 8b is achieved by means of *ionic two parameter* potentials.

7.5.2 Calculation of α_e and $\omega_e x_e$ for 308 Bonds

A calculation of the constants α_e and $\omega_e x_e$ directly from the potentials gives the results collected in Table 4, given in Supporting Information.

Only for α_e , we tried to present the results graphically (see Figure 9a), using a log scale due to the large differences in α_e values. Two help-lines are drawn at $\pm 25\%$ of the experimental α_e values. Help-lines at a lower percentage interfere too much with the empirical fittings through the origin (-20% would nearly coincide with the Morse trendline, whereas $+10\%$ or $+15\%$ would have been too close to the Kratzer trendline). For 308 bonds, the mean deviation for the Kratzer I potential is 18.1% and for Morse's 20.1% (see also Table 4). This makes the performance of the two comparable but the errors are too large for a universal potential.

We must however divide these 308 bonds in two main series:

- 197 bonds with at least one monovalent atom and a main column element
- 111 other bonds, including bonds between polyvalent atoms, Van der Waals molecules, ...

This distinction is necessary since we can expect that only with A' near or equal to 1, the Kratzer I asymptote can reasonably be calculated without any further assumptions. For these 197 *simple* bonds, it can be expected that also Morse's function will behave at its best. Part one of Table 4 in the Supporting Information (197 bonds) reveals that the performance of the two parameter Kratzer potential with a *wrong* asymptote is now significantly better than Morse's three parameter potential, which uses the natural and *correct* asymptote.

Table 5a gives an overview of the spread of the mean deviations (%) in the 197 and 111 series. It is easily verified that the Kratzer potential is superior to Morse's for pre-

Table 4. Data for 308 bonds (sample for 27 bonds from part one: 197 bonds containing at least one mono-valent atom)^[a]

Nr	Bond	Col Class	$\omega_e x_e$ (exp)	$\omega_e x_e$ Kratzer	$\omega_e x_e$ Morse	% $\omega_e x_e$ Kratzer	% $\omega_e x_e$ Morse	α_e (exp)	α_e Kratzer	α_e Morse	% α_e Kratzer	% α_e Morse	C	abs% C	F	G
1	Cs ₂	1A1A	0.0823	0.05	0.14	−44.9	68.7	0.0000264	0.000027	0.000053	1.0	101.5	1.061	21.6	1.145	51.84
2	K ₂	1A1A	0.328	0.20	0.51	−40.3	56.9	0.000212	0.000237	0.000424	11.7	99.9	1.042	22.9	1.034	46.70
3	Li ₂	1A1A	2.61	2.08	3.66	−20.1	40.3	0.00704	0.007939	0.010294	12.8	46.2	1.409	4.2	0.911	31.03
4	LiNa	1A1A	1.612	1.20	2.38	−25.7	47.9	0.0036	0.003678	0.005312	2.2	47.6	1.448	7.1	0.983	32.46
5	Na ₂	1A1A	0.72547	0.49	1.09	−32.9	50.3	0.0008736	0.000940	0.001493	7.6	70.9	1.239	8.4	0.968	37.50
6	NaK	1A1A	0.511	0.32	0.77	−37.2	50.8	0.0004584	0.000455	0.000759	−0.8	65.6	1.230	9.0	1.158	45.15
7	LiO	1A6	12.5	7.66	6.45	−38.7	−48.4	0.0151	0.018179	0.013383	20.4	−11.4	0.856	36.7	1.483	83.09
8	CsBr	1A7	0.374	0.38	0.17	0.3	−55.5	0.000124012	0.000130	0.000060	4.5	−51.7	1.376	1.8	2.378	82.93
9	CsCl	1A7	0.731	0.75	0.31	3.2	−57.5	0.00033756	0.000363	0.000157	7.6	−53.6	1.372	1.5	2.318	81.10
10	CsF	1A7	1.615	1.91	0.75	18.5	−53.7	0.00117562	0.001435	0.000587	22.1	−50.1	1.392	3.0	2.032	70.06
11	CsI	1A7	0.2505	0.24	0.12	−3.1	−50.6	0.000068263	0.000069	0.000036	1.5	−47.0	1.375	1.7	2.429	84.79
12	KBr	1A7	0.8	0.72	0.36	−10.2	−55.0	0.00040481	0.000415	0.000205	2.6	−49.3	1.327	1.8	2.178	78.78
13	KCl	1A7	1.3	1.21	0.56	−7.3	−56.6	0.0007899	0.000820	0.000386	3.8	−51.1	1.327	1.8	2.236	80.83
14	KF	1A7	2.4	2.63	1.12	9.5	−53.3	0.002335038	0.002552	0.001099	9.3	−52.9	1.488	10.0	2.126	68.57
15	KI	1A7	0.574	0.55	0.32	−3.5	−43.4	0.00026776	0.000272	0.000157	1.6	−41.5	1.429	5.7	2.246	75.68
16	LiBr	1A7	3.53	3.83	2.27	8.6	−35.7	0.0056442	0.006209	0.003358	10.0	−40.5	1.621	19.9	1.717	50.83
17	LiCl	1A7	4.501	4.84	2.65	−7.4	−41.1	0.00800961	0.008741	0.004362	9.1	−45.5	1.620	19.8	1.720	50.95
18	LiF	1A7	7.929	8.72	4.35	10.0	−45.2	0.0202826	0.021569	0.009512	6.3	−53.1	1.731	28.0	1.700	47.14
19	LiI	1A7	3.39	3.12	2.17	−8.0	−35.9	0.00409	0.004528	0.002873	10.7	−29.8	1.356	0.3	1.729	61.18
20	NaBr	1A7	1.5	1.23	0.76	−17.9	−49.6	0.00094095	0.000960	0.000562	2.0	−40.3	1.253	7.3	2.071	79.31
21	NaCl	1A7	2.05	1.77	0.98	−13.8	−52.1	0.00162482	0.001643	0.000874	1.1	−46.2	1.330	1.6	2.084	75.19
22	NaF	1A7	3.4	3.54	1.67	4.1	−50.8	0.00455869	0.004502	0.002042	−1.2	−55.2	1.645	21.7	2.133	62.24
23	NaI	1A7	1.08	0.93	0.69	−13.8	−36.3	0.00064777	0.000669	0.000457	3.3	−29.4	1.314	2.8	2.007	73.32
24	RbBr	1A7	0.463	0.46	0.23	−0.4	−50.7	0.00018596	0.000190	0.000095	2.1	−48.8	1.432	5.9	2.325	77.91
25	RbCl	1A7	0.92	0.83	0.37	−10.1	−59.6	0.00045365	0.000471	0.000214	3.9	−52.9	1.283	5.1	2.244	83.96
26	RbF	1A7	1.9	2.09	0.88	9.8	−53.9	0.00152279	0.001704	0.000736	11.9	−51.6	1.430	5.8	2.150	72.13
27	RbI	1A7	0.335	0.31	0.18	−6.1	−46.2	0.00010946	0.000110	0.000063	0.5	−42.7	1.378	2.0	2.344	81.60

^[a] The complete Table 4 is available as “Supporting Information”.

Table 5a Number of bonds in groups of mean %-deviations by number of bonds, by constant, by potential, by series (197 or 111)

Constant	Potential	series # bonds	# with 0–5%	# with 5–10%	# with 10–15%	# with 15–20%	# with 20–30%	# with 30–40%	# with 40–50%	# with 50–100%	# with ≥100%
α_e	Kratzer	197	85	41	28	15	19	7	1		1
α_e	Morse	197	31	28	23	17	37	23	17	20	1
α_e	Kratzer	111	5	14	7	9	18	33	6	18	1
α_e	Morse	111	20	30	24	11	19	3	3	1	
$\omega_e x_e$	Kratzer	197	49	38	25	31	35	10	6	3	
$\omega_e x_e$	Morse	197	22	32	24	19	28	24	16	30	2
$\omega_e x_e$	Kratzer	111	6	14	14	14	19	17	9	14	4
$\omega_e x_e$	Morse	111	26	12	13	12	28	12	5	3	

Table 5b. Column classification of 197 bonds with at least one monovalent atom: mean deviations for calculated α_e and $\omega_e x_e$ values with the Kratzer (I) and the Morse potential

Column 1	Data/Column 2	1	2	3	4	5	6	7	H	Total
1	Nr	9	2	2		1	4	28		46
	% α_e (Kratzer I)	9.86	3.16	10.02		4.73	15.61	5.39		7.24
	% α_e (Morse)	50.63	4.28	12.07		15.74	7.59	37.45		34.42
	% $\omega_e x_e$ (Kratzer I)	33.43	7.47	22.32		33.54	28.20	8.98		16.48
	% $\omega_e x_e$ (Morse)	38.00	9.36	10.23		11.47	19.43	38.75		33.81
7	Nr		10	22	8	8	4	12		64
	% α_e (Kratzer I)		19.11	10.35	10.88	6.68	13.05	6.02		10.68
	% α_e (Morse)		28.72	28.46	13.65	7.61	46.80	26.52		24.83
	% $\omega_e x_e$ (Kratzer I)		25.85	9.36	7.81	9.06	26.18	22.95		15.30
	% $\omega_e x_e$ (Morse)		26.67	24.57	13.25	16.12	84.03	37.14		28.50
H	Nr	13	19	9	8	5	7	18	8	87
	% α_e (Kratzer I)	8.73	17.02	6.70	3.19	5.32	8.15	9.11	15.08	10.24
	% α_e (Morse)	5.36	36.74	8.23	10.64	12.25	17.35	13.10	25.13	17.78
	% $\omega_e x_e$ (Kratzer I)	9.95	16.85	16.15	17.90	16.73	19.89	7.33	6.15	13.13
	% $\omega_e x_e$ (Morse)	13.25	44.29	13.31	20.95	21.97	16.12	15.23	7.46	21.35
Nr		22	31	33	16	14	15	58	8	197
	% α_e (Kratzer I)	9.19	16.80	9.34	7.04	6.06	11.44	6.67	15.08	9.68
	% α_e (Morse)	23.88	32.06	21.95	12.15	9.85	22.60	27.63	25.13	23.95
	% $\omega_e x_e$ (Kratzer I)	19.56	19.15	11.99	12.85	13.55	23.78	11.36	6.15	14.62
	% $\omega_e x_e$ (Morse)	23.38	36.35	20.63	17.10	17.88	35.11	31.12	7.46	26.56

dicting the two constants in 197 series. The number of bonds in the 0–10% range is twice as large for the Kratzer potential, 126 and 86, than for Morse's, 59 and 54 respectively.

The first row of data in Table 5a shows that up to bond number 85, the average deviation is $\pm 2.38\%$. Up to number 126, it is $\pm 3.97\%$, up to 154 $\pm 5.41\%$, up to 170 $\pm 6.47\%$ and up to 188 $\pm 8.08\%$ (for bond 197 it is 100%). As we pointed out above that an average error of about $\pm 5\%$ can be considered as a reasonable limit for a “universal potential”, the Kratzer–I–Varshni–V potential seems to meet this criterion and is certainly superior to Morse's.

Error ranges derived from the square root of the percentage deviation for α_e times that for $\omega_e x_e$ for the same bond in the same 197 series give

– Kratzer potential deviation $\pm 20\%$ 171 bonds; $\pm 10\%$ 128; $\pm 5\%$ 57

– Morse potential deviation $\pm 20\%$ 109 bonds; $\pm 10\%$ 62; $\pm 5\%$ 20.

With this criterion, Kratzer's potential is again superior to Morse's. With Kratzer's potential, the deviation for 171 bonds (i.e. 87% of 197 bonds) is $\pm 7\%$ for α_e and $\omega_e x_e$ combined.

In order to get an idea of the regularities in these results, we arranged all 308 bonds according to a rough Column

classification, e.g. NaK in 11, RbF in 17, BeCl in 27, ... We also computed C (the Calder–Ruedenberg constant) and its % deviation from the average value. F and G values are also given. Table 4 (Supporting Information) gives these additional results for all 308 bonds, divided in the 2 series, ordered by a Column classification and alphabetically by bond.

A global comparison of the performances of the Kratzer and Morse potentials for calculating α_e and $\omega_e x_e$ for the 197 simple bonds is given in Table 5b, using the Column classification as a guideline. The % deviations for the Kratzer potential are smaller than those obtained with the Morse potential. Only rarely, one observes a better score for the Morse potential. The Morse results found here are slightly better than those reported by Varshni, who qualified this potential as not too good.

In the 23 bonds used by Varshni^[3] 17 would belong to the 197 series and his results are $\pm 36.4\%$ for α_e and $\pm 32.9\%$ for $\omega_e x_e$ (for 23 bonds: he found deviations of 33.1% and 31.2% respectively). Varshni's best results were obtained with an *empirical* potential. The 23-bond set gave errors of $\pm 22.1\%$ for α_e and $\pm 11.1\%$ for $\omega_e x_e$. The figures for the 17 bonds set are nearly the same and comparable with those in Table 5b.

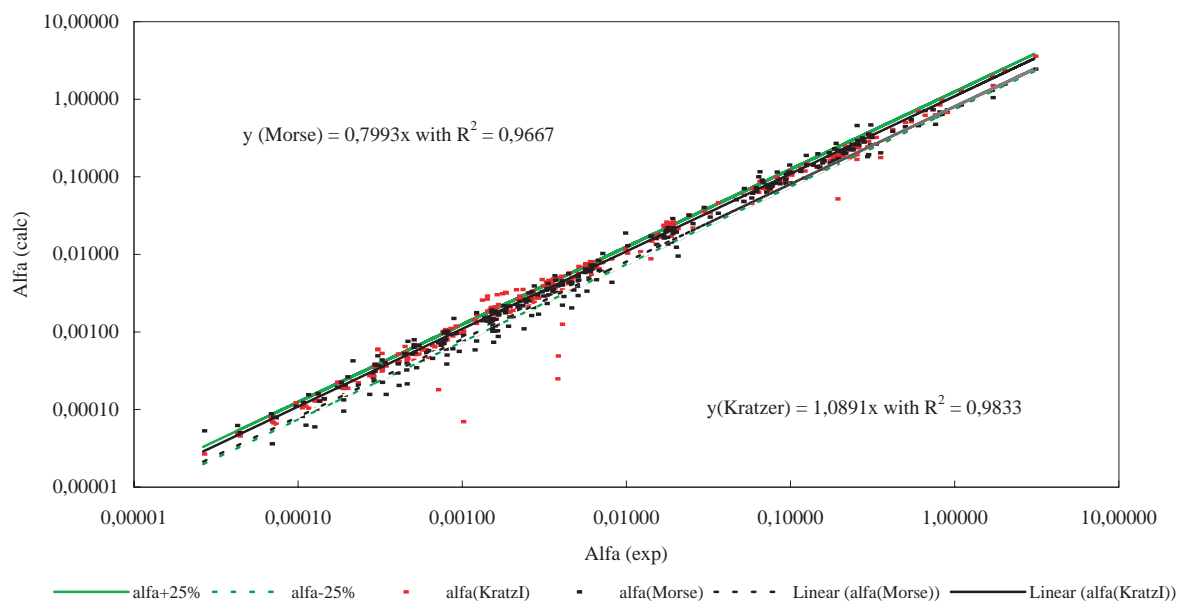


Figure 9a. Alfa for 312 diatomics, computed from Kratzer I/Varshni V and Morse potentials

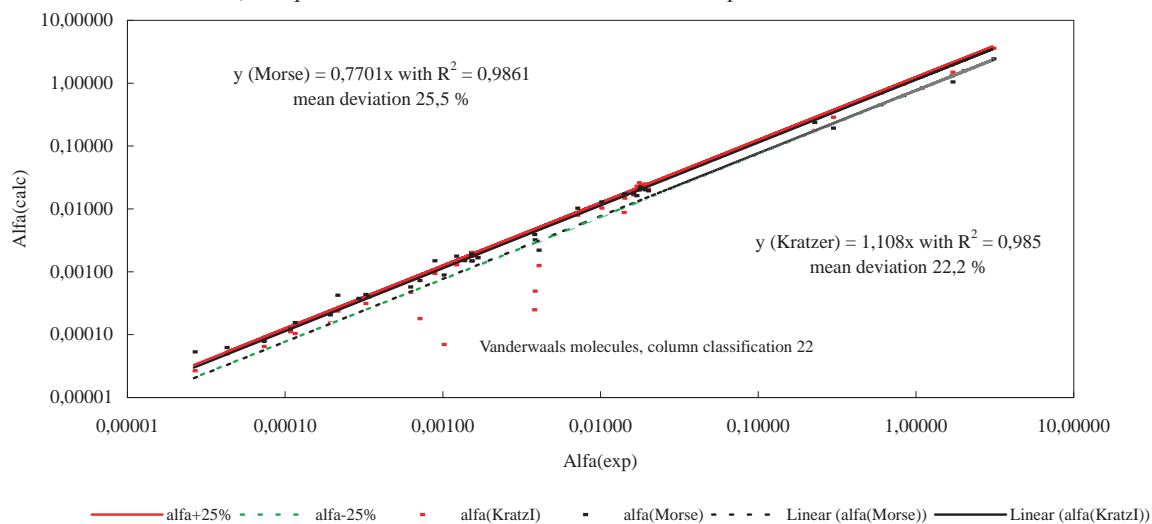


Figure 9b. Alfa for 42 homonuclear bonds, computed from Kratzer I/Varshni V and Morse potentials

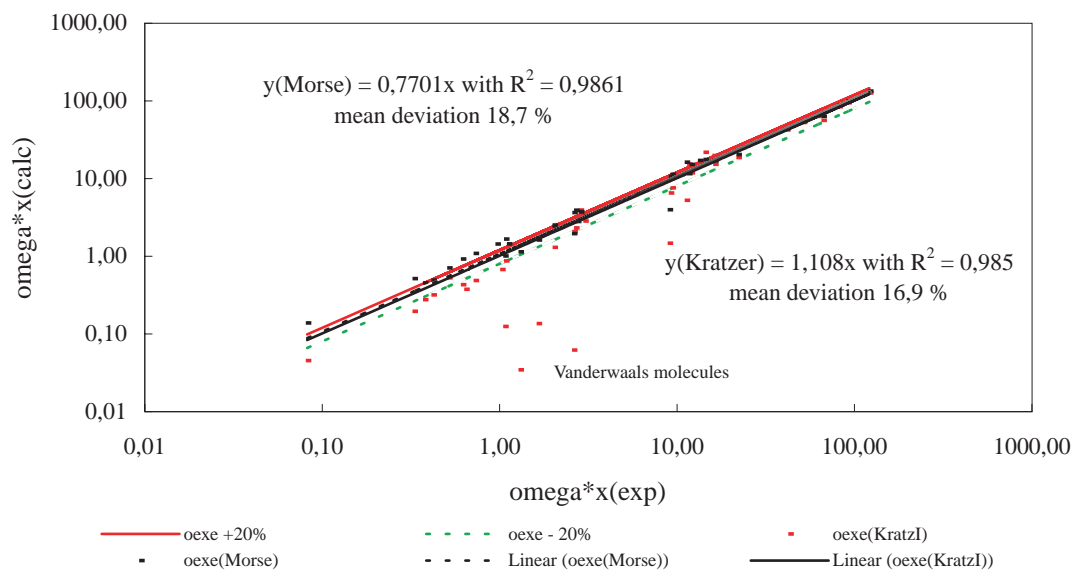


Figure 9c. Omega*x for 42 homonuclear bonds, computed from Kratzer I/Varshni V and Morse potentials

With respect to the Morse results, mean deviations in % are 2 to 3 times smaller for the Kratzer potential (Table 5b). We must keep in mind that many of the compiled constants are uncertain, not all equally accurate and sometimes even in error: the experimental α_e value for YCl (bond Nr. 77 in Table 4) is probably not correct.

Part two of Table 4 reveals interesting further details on this subject. For these 111 bonds, the situation is opposite in terms deviations. Now, Morse's potential seems superior to Kratzer's. However, the overall result for the 308 bonds is slightly in favor of the Kratzer potential again. However, this is not straightforward an interpretation.

In fact, the largest deviations for the Kratzer I potential in the 111 bonds set are found

(a) for cases in which $A \ll 1$ (Van der Waals molecules in group 22 and bonds with noble gas elements in group O): here all deviations are *negative and very large* (between 50 and 100%), meaning that the ionic limit is *overestimated* with an A value around 1

(b) for cases in which $A \gg 1$ (multiple bonds): here the opposite situation applies, since all deviations are now *positive and large* ($> 20\%$), as expected. Here the ionic limit is clearly *underestimated*. Numerical results are shown in Tables 4–5.

We did not want an empirical parameterization of the results (for instance using coefficients of empirical trend-lines produced in the plots instead of their theoretical values^{[2][3]}). In many cases, this would improve the results empirically (smaller % deviations).

7.5.3 Calculation of α_e and $\omega_e x_e$ for 43 Homonuclear Bonds

With Varshni,^[3] we do not understand why the Morse potential has such a good reputation, especially for covalent bonds, as mentioned in many textbooks. Therefore, we selected data for homonuclear diatomics and compared the performances for this type of bond (43 bonds are available, polyvalent atoms, molecular ions, noble gases, ... are all included, see Table 4, Supporting Information).

We present the results in Figure 9b for α_e with the rather surprising conclusion that even here the mean deviations for the ionic Kratzer I potential are smaller than for Morse's covalent potential. Nevertheless, 5 Van der Waals bonds are included (for which the ionic potential with $A = 1$, $I = 0$, underestimates these asymptotes). These points are indicated in Figure 9a.

In addition, for $\omega_e x_e$ (see Figure 9c) a similar situation applies. Despite the large deviations from $A = 1$ (both > 1 and < 1), exactly as in the 111 series and despite the wrong asymptote, the performance of the Kratzer potential is still comparable with that of Morse's for 43 homonuclear bonds. This is a surprising and unexpected result.

7.5.4 Calculation of α_e and $\omega_e x_e$ for 91 Single Bonds

For 91 bonds between two monovalent atoms, interesting details show (Table 4, Supporting Information). We refer for this set also to Figure 2, Figure 8, and Figure 7c. The global results are:

- Kratzer potential: mean % deviation for $\alpha_e \pm 8.2$, for $\omega_e x_e \pm 13.16\%$
- Morse potential: mean % deviation for $\alpha_e \pm 25.9$, for $\omega_e x_e \pm 26.54\%$.

These deviations are, as expected, even more pronounced and again in favor of the Kratzer-I–Varshni V potential (see also Tables 5a–b).

7.5.5 Conclusion of This Section

It is difficult to visualize all the results obtained thus far, due to large differences in magnitude, as in Figure 9a–b–c. Nevertheless, we can safely conclude that

(a) an ionic function is better than a covalent one and especially that

(b) the Kratzer-I–Varshni V potential is the most likely candidate, if any, for being a *two-parameter* universal potential.

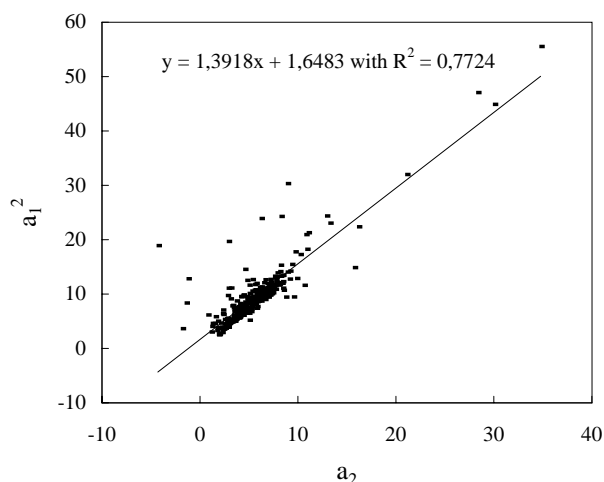
We will try to illustrate these differences graphically using the Graves–Parr scaling method.^[2]

7.6 Scaling 300 Pairs of Dunham Coefficients with an Ionic Sutherland Parameter in the Graves–Parr Scaling Hypothesis

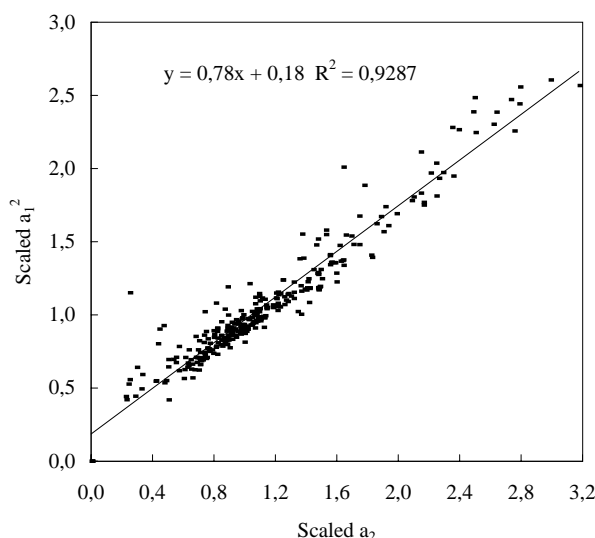
The failure of the Graves–Parr scaling hypothesis led these authors to conclude that this is a deciding step towards the determination of a *four-parameter potential*.^[2] Our thesis is to abandon simply the covalent Sutherland parameter as a species dependent scale factor. We can indeed easily demonstrate that the mathematically correct Graves–Parr scaling hypothesis is valid, contrary to their own conclusion, and, hence, that a fourth parameter is not necessary at all.

Let us first give a picture of the unscaled a_1^2 and a_2 values for 381 bonds (Figure 10). Graves and Parr used 150 bonds, leading to a maximum value of the coordinates of 17 for y and 11 for x , considerably lower than those appearing in Figure 10. The empirical fit gives a coefficient of 1.4, within 6% of the coefficient predicted by the Kratzer potentials (Table 2). Even the Kratzer potential, with *ideal* Dunham coefficients (Equation 15), is in line. The most important feature of this Figure 10 is that this scale enlargement to 381 bonds already leads to a rough *clustering*, in agreement with the Graves–Parr scaling hypothesis, and contrary to their own observation, which mentions only *scattering*.^[2]

Scaling the coefficients with the covalent Sutherland parameter reduces the number of available data to 303, as D_e must be available. Figure 11 gives the result after scaling with the three parameter Morse potential. The slope is near

Figure 10. Unscaled a_1^2 versus unscaled a_2 for 381 bonds

unity for a trend line through the origin and the fit of 0.9 is better than in Figure 10 (but this could also be due to a statistical effect, not mentioned by Graves and Parr). Theoretically, at least according to the Graves–Parr^[2] scaling hypothesis, the slope should not only be unity but all data points should focus (*cluster*) at a locus near $x = 1$, $y = 1$. This is apparently not the case (see Figure 11).

Figure 11. Scaled a_1^2 versus scaled a_2 (covalent Sutherland parameter, D_c) for 312 bonds

We do not show the result for scaling with the Kratzer II potential but immediately give the plot in Figure 12, resulting from scaling with the ionic Sutherland parameter (Kratzer–I–Varshni–V two parameter potential). Since we are no longer dependent on the availability of D_c (just R_c is sufficient), we could at the same time have treated the 381 bonds in Figure 10. However, we wish to compare the two potentials under review by a one by one method. Therefore the same set of 303 bonds is analyzed as in Figure 11 and the same scale is retained to make the differences more pronounced. In comparison with Figure 11, we observe a considerable improvement. This shows above all in the clus-

tering of the data-points in the range $0.8 < x < 1.2$ and $0.8 < y < 1.2$, which is to be expected if the Graves–Parr scaling hypothesis is valid. The slope is near unity but the fit is less than in Figure 11 (which could be a normal consequence of more intensive clustering).

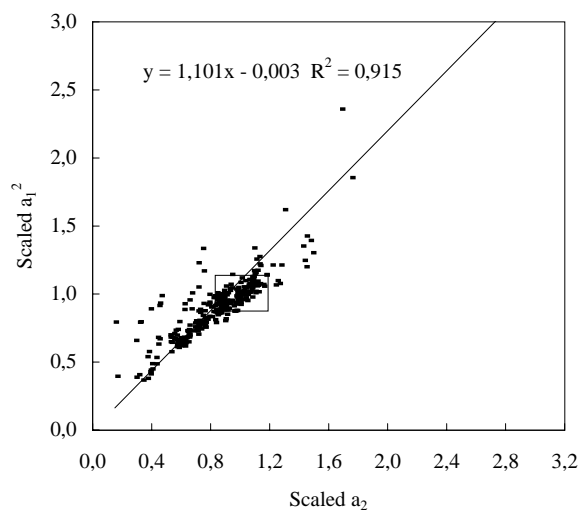
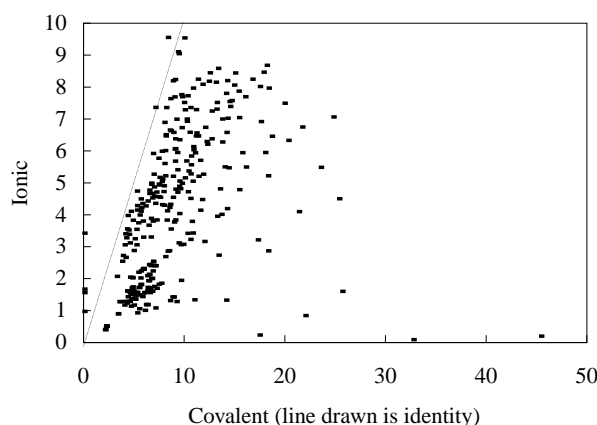
Figure 12. Scaled a_1^2 versus scaled a_2 (ionic Sutherland parameter, e^2/R_c) for 312 bonds

Figure 13. Plot of covalent versus ionic Sutherland parameter for 312 bonds

All this is the more remarkable since the covalent Sutherland parameter values are, on average, *twice as large* than the ionic ones. To illustrate this, we made a plot of the two Sutherland parameters in Figure 13. Scaling by *larger* values should automatically compresses the scaled data to *smaller* values, whereas exactly the opposite effect is observed: the scaling operation is more effective using smaller scaling factors (ionic Sutherland parameters). Considering this shows that the scaling/clustering is even more effective than one could conclude from a simple comparison of the two Figures 11 and 12.

In Figure 14–15, we present the results for the 91 bonds between monovalent atoms. The Morse Graves–Parr plot, Figure 14, does not differ significantly from the general one, Figure 11. For just 22 out of 91 bonds, the data cluster in the critical box. On the contrary for the ionic potential in

Figure 15, the opposite result is obtained: only 21 data points are outside the critical range near $x = 1, y = 1$, the most important deviation being found for F_2 , indicated in Figure 15. We cannot but conclude that the Graves–Parr scaling hypothesis is indeed valid, contrary to their conclusion. However, this only shows when an alternative asymptote acts as a species dependent scaling factor.

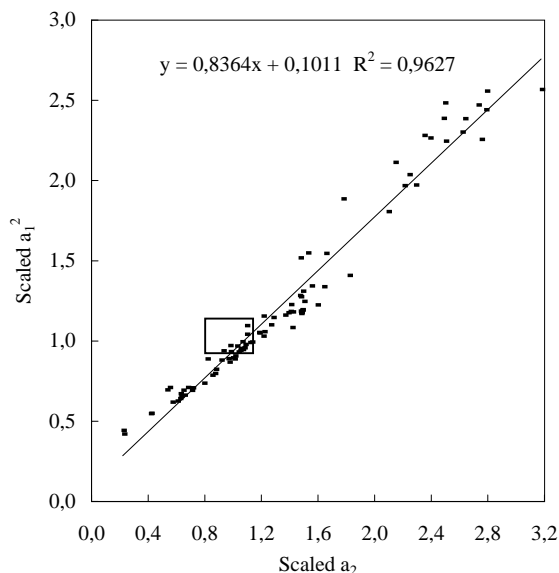


Figure 14. Scaled a_1^2 versus scaled a_2 (covalent Sutherland parameter, D_e) for 91 single bonds

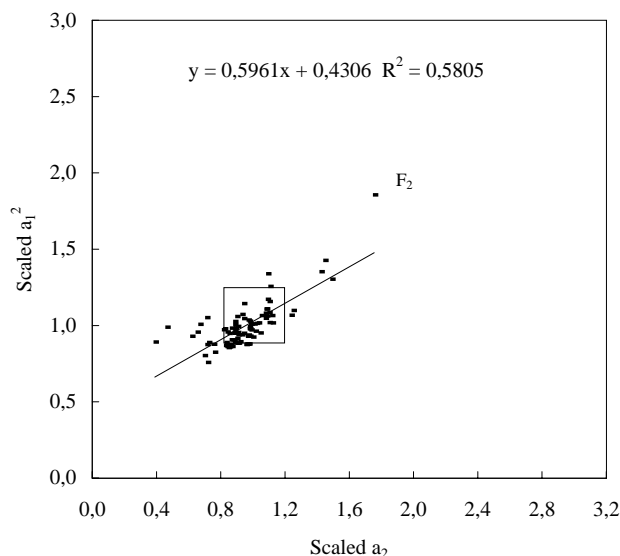


Figure 15. Scaled a_1^2 versus scaled a_2 (ionic Sutherland parameter, e^2/R_e) for 91 single bonds

We had to diverge on this aspect not only for important theoretical but also for practical reasons. Normal graphical procedures are difficult to apply for data, extending to several powers of 10 for a large number of cases (see above, Figure 9a–c and the data in Table 4).

The last figure in this section, Figure 16, represents the scaling results, using the generalized Kratzer–I–Varshni–V potential. This is the only potential giving the theoretical

result that $\Delta^{1/2} = F$. This result must be compared with Figure 12.

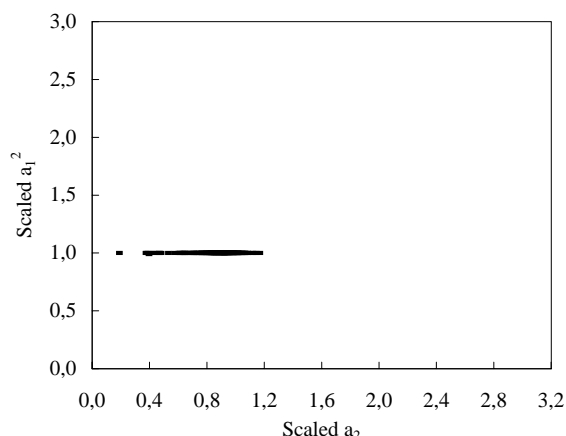


Figure 16. Scaled a_1^2 versus scaled a_2 (Kratzer result, Sutherland parameter = F^2) for 312 bonds

Scaling is now *of course perfect* for a_1^2 but a spread remains for a_2 , although 244 data points out of the 303 are still within the critical box (now line) near unity. The concentration of 244 data-points in Figure 16 between 0.8 and 1.2 on the x -axis and an average value for the scaled a_2 of 0.859, i.e. $1 \pm 14\%$, for the 303 bonds indicates that the Kratzer–I–Varshni–V potential is quite effective but not completely exact. The spread in the scaled a_2 values is due in the first instance to a scattering in G/F values. Maybe, the Dunham series is in need of revision (possibly with respect to the truncation of the series for the vibrational energy given the relatively small average deviations on the x -axis or, maybe, higher order Dunham coefficients are needed). Maybe also asymptote differences (and hence the critical distance) come into play.^[7]

Introducing a third parameter in the Kratzer–I–Varshni–V function might improve the scaling operation and its universal characteristics. Unlike Graves and Parr, we conclude that a four-parameter function is not necessary to obtain better scaling. The large number of data used is an extra argument for this conclusion. Finally, Figure 16 can only be reproduced from ionic potentials as soon as we can show how the identity $F = \Delta^{1/2}$ can be obtained from our scheme for *all* molecules, i.e. those including $A \neq 1$.

7.7 Extension of the Predictions to All Molecules

We now proceed to the necessary, be it totally empirical, extension of the results obtained thus far to all bonds. We can apply a classification scheme (Calder–Ruedenberg^[5] or Herschbach–Laurie^[19]). A classification in either way is like adding an additional third (but not quantified) parameter. We therefore constructed a pivot table with the Column classification as a guideline and calculated mean A factors in Equation (28) using the Kratzer–I–Varshni–V potential and experimental F values. We wish to restrict the number of A values to a minimum and require that they should be not too far from 1 in all cases, where at least *one monovalent atom* is present. With two polyvalent atoms in

Table 6. Mean values of $F(\text{calc})/F$, absolute% deviations and mean C values for 269 bonds with 7 different A values (Column classification) monovalent-monovalent monovalent-polyvalent polyvalent-polyvalent

Groups	H1	H7	H H	11	17	7 7	H2-6	1.2-6	27	37	4 7	5 7	6 7	26	33	3.5-6	44	4.5-6	5 5	5 6	6 6	Total	
A value or Mean																							
0.8		2		2			5	1														10	
F(calc)/F		0.956		0.984			1.021	1.014														1.006	
abs%F		4.41		2.70			3.37	3.28														3.32	
C		1.751		1.302			1.685	1.410														1.560	
0.9	#	4	1	1	2	1	10	3	1		1	3	3			1				1		32	
F(calc)/F		1.029		0.989	0.997	1.023	1.014	1.027	1.016	0.959	1.037	1.009	0.998			0.971				1.022	1.015		
abs%F		2.92		1.14	0.28	2.39	1.39	2.74	4.38	4.10	3.66	3.08	0.66			2.88				2.20	2.62		
C		1.638		1.956	1.173	1.387	1.063	1.579	1.424	0.932	1.530	1.515	1.241			1.848				1.264	1.482		
1.0	#	2	5	1	3	18	10	19	3	18	3	3							1	3	89		
F(calc)/F		0.992	1.014	0.975	1.008	1.003	0.987	0.999	1.007	1.005	1.004	0.980								0.971	1.044	1.001	
abs%F		0.77	2.51	2.47	1.32	2.66	2.69	2.31	3.17	2.35	1.77	2.03								2.88	4.40	2.45	
C		1.578	1.588	1.783	1.246	1.406	1.207	1.597	1.264	1.469	1.437	1.462								1.157	1.371	1.444	
1.1	#	5	11	3	7		6	3		2	2			2	2	2	1	1		2	2	51	
F(calc)/F		0.990	1.000		1.000	0.993	1.003	1.001		0.966	0.999			1.004	0.968	0.966	1.038	1.039		0.962	1.009	0.995	
abs%F		2.91	2.38		1.69	1.33	2.40	1.70		3.44	1.32			2.70	3.17	3.44	3.80	3.92		3.82	1.28	2.37	
C		1.688	1.627		1.230	1.517	1.486	1.459		1.541	1.482			1.302	1.155	1.231	1.429	1.269		1.258	1.367	1.477	
1.2	#	2	1	6	1		5	1	4	1			1	2			4	3	5	4		40	
F(calc)/F		0.991	0.983	0.982		1.018	1.017	1.003	0.993	1.003	1.013	1.029					1.009	1.003	0.996	0.994	1.000		
abs%F		2.12	1.73	1.78		1.75	1.68	0.32	1.64	0.32	1.29	2.89					2.19	2.18	1.97	2.72	1.93		
C		1.595	1.539	1.801		1.392	1.439	0.856	1.525	1.390			1.755	1.302			1.253	1.149	1.310	1.377	1.434		
1.3	#							1	1	2			3			1	11	2	1	2	24		
F(calc)/F								1.003	0.970	1.010			1.005			1.013	1.006	1.016	0.964	0.971	1.001		
abs%F								0.31	3.03	1.12			2.14			1.32	1.73	1.60	3.59	2.91	1.87		
C								1.366	1.304	1.144			1.222			1.424	1.260	1.301	1.409	1.205	1.264		
1.4	#						3	1	1							2	2	8	4	2	23		
F(calc)/F							0.977	1.000	0.989							1.014	0.977	0.997	0.977	0.975	0.988		
abs%F							2.34	0.02	1.15							1.37	2.31	1.99	2.31	2.53	1.99		
C							1.495	1.456	1.417							1.482	1.409	1.403	1.252	1.359	1.395		
Total	#	13	18	8	9	28	48	9	10	21	8	8	4	7	2	6	3	24	9	11	12	269	
F(calc)/F		1.003	1.001	0.982	0.999	1.003	0.990	1.008	1.011	0.994	1.002	1.000	0.995	1.001	1.011	0.968	0.990	0.997	1.005	0.994	0.981	1.007	1.001
abs%F		2.46	2.49	1.79	1.63	2.28	2.57	2.46	3.28	1.61	2.23	2.26	2.25	0.82	2.51	3.17	2.30	2.81	1.98	2.11	2.64	2.89	2.32
C		1.641	1.618	1.818	1.245	1.432	1.194	1.566	1.304	1.423	1.455	1.402	1.487	1.370	1.268	1.155	1.450	1.416	1.307	1.229	1.304	1.336	1.437
Ions	#		5	2		2	11										1	2	2	1	1	27	

a bond, larger deviations for A from unity can be expected. These would then have to follow roughly the Calder–Ruedenberg classification,^[5] if this makes sense. These authors, with Graves and Parr,^[2] used 13 groups (13 values for the additional but hidden parameter) in their analyses of 150 molecules, of which some classes are very similar and nearly coincide (see also Figure 1b).

Table 6 gives the results. Only seven different (rounded) A values are needed to encompass the results for 269 bonds (in which 27 molecular ions are included, see bottom line of Table 6). The %-deviations of the experimental F values are given, as well as the mean C value for each class. The correlation with the Column classification is roughly followed for polyvalent atoms but we do not discuss the details. We observe that an ionic three-parameter potential is largely sufficient. In addition, just 5 A parameters around unity, i.e. 0.8; 0.9; 1.0; 1.1, and 1.2 account for more than 220 of the 269 bonds, covering F to within $\pm 3\%$ (and hence also α_e).

Obviously, a three parameter ionic potential is capable of producing Figure 16, which is the best scaling result yet obtainable for the Dunham coefficients a_1 and a_2 . This is based upon the identity $F = \Delta^{1/2}$, which is also generated by the generalized Kratzer–I–Varshni–V potential.

7.8 G/F (Calder–Ruedenberg Constant C) and $G/(1 + F)^2$ Values

The C ratio's in Tables 4–6 reveal that the mean deviation is about the same as for α_e computed with the

Kratzer–I–Varshni–V potential. For the corresponding G/F values in function of F , the observed spread (not shown) is 3 times larger than for the $G/(1 + F)^2$ values. This leads us again to conclude that C is far from being constant (see above). However, it is difficult to find any regularity in G/F values (C values) or in $G/(1 + F)^2$ values. This remains the largest stumbling block in achieving a complete picture in the spectroscopic behavior of molecules in terms of ionic potentials or of any kind of potential. The scattering in the G/F ratio is also responsible for the scattering in the scaled a_2 values in Figure 16. Reminding the definition of G/F (or C), in Equation (30), all this must not come as a surprise.

Preliminary analyses point in the direction of a possible relation of the G/F - or similar ratio's with the critical distance (which corresponds with the asymptote difference). Although this sounds logical^[7] and in line with the possible interference of the non-crossing rule (see above), a further discussion of this important question is not given, as more work is needed.

7.9 The Existence of a Universal Two-Parameter Function: Alternative Choices

Against all expectations in the literature, the $F(\Delta)$ - and $G(\Delta)$ relations and the scaling effects of an ionic Kratzer–I–Varshni–V potential upon a_1 and a_2 indicate that even a universal two-parameter function does exist for the situation around R_e for a large number and variety of bonds. In addition, its performances for reproducing first order constants are excellent. Using a third parameter for this

function results in an exact fit, as far as F is concerned (see Table 6) and, hence, in almost perfect scaling (as depicted in Figure 16) with a small number (7) of A values for 269 bonds. This corresponds with a really universal three parameter potential.

However, speaking of two or three parameters has become somehow confusing, since we disregarded constraint (ii). But, to put all functions on an equal basis, other functions should be tested upon their relative merits for coping with the constants, using for scaling, instead of D_e , the asymptote generated by the function itself (an example was given by Von Szentpaly^[15]).

We cannot predict the outcome of such a review, although we tested here two important *reduced* functions, belonging to two completely different classes of potentials (Morse, exponential and of covalent type versus generalized Kratzer, Coulomb-like and of ionic type). However, a better low parameter potential may appear for scaling purposes. Then, one must review also its capacity (a) to explain chemical bonding (at the minimum) and/or (b) to reproduce the atomic dissociation limit.

In this last respect, any ionic potential will fail by definition as will any other potential with an asymptote $D_x \neq D_e$. In fact, under the rather severe simplifying conditions inherent to ionic potentials and without the condition that D_e should be reproduced, the deviations found in $G(F)$ plots as well as those found in $G/F(F)$ plots indicate that inconsistencies remain with ionic and, most probably, also with a number of other potentials. These can be due either to (a) errors in experimental data (not taken into account), (b) the choice of the potentials (and their analytical form), (c) the Dunham expansion (in which higher order terms in the vibrational part are neglected), (d) higher Dunham coefficients (not considered here^{[2][24]}) or finally to (e) a discontinuous switch between dissociation limits at an R value $\infty > R > R_e$, whereby there is a corresponding shift from one potential to another or from one set of parameters to another in the same potential (non-crossing rule, see next section).

7.10 Obtaining the Correct or Atomic Dissociation Limit, Using an Ionic Two-Parameter Potential

The inconsistencies observed for scaled a_2 values (or in G and in G/F ratios and related ones) indicate that away from the minimum other corrections or additional coefficients are needed for the situation at $R \gg R_e$. As the ionic asymptote is situated between a_0 and D_e , the non-crossing rule can interfere.

For large R , interatomic forces are commonly designed as Van der Waals-forces, varying with $1/R^n$, with $n > 2$, which are not point charge Coulomb forces^[39] as the ones leading to the *ionic* dissociation limit. Very recently, a possible switch from an ionic (Kratzer) potential to a covalent one somewhere between R_e and ∞ was described by Herrick and O'Connor.^[40] The problem is not discussed here in detail, as, with Graves and Parr,^[2] we remain convinced that the

primary evidence about the relations between the constants and even about convergence is to be found in the first constants in the Dunham expansion and to the (analytical form of the) potential, wherein R_e , k_e and the asymptote (be it D_e or D_x) will invariantly play a crucial role.

But, these important further details must not distract us from the main conclusion *that a universal two-parameter ionic function exists within reasonable limits*.

7.11 Chaotic/Fractal Behavior

Although we present evidence that Coulomb's (inverse power) law is important for understanding the relations between the constants of a large number of molecules, this does not fully support fractal/chaotic behavior in anharmonicity.^[16] The evidence presented thus far^[16] is not yet convincing. We found that power relations in some critical cases are not significantly better than classical linear or quadratic relations. We showed that the use of power laws can be misleading, as fundamental details can get lost (the breaking of the $M-Z$ symmetry). Using log-scales may be an aid when scale differences get large, but they do not change the underlying physical or chemical ideas.

7.12 A Universal Bond, Atomic and Molecular Spectroscopy

Finding a universal function is equivalent to finding a universal bond, a standard for molecular spectroscopy, and the equivalent of H , the standard for atomic spectroscopy.

The Kratzer potential is also applicable in atomic spectroscopy.^[34] In molecular spectroscopy, a *one parameter potential* reduces to $U(R) = (e^2/R_e)(1 - R_e/R)^2$ and leads to $\Delta^{1/2} = 1$ (or $F = 1$). Then the most likely candidate for a universal bond should obey almost all of the following constraints to within reasonable limits: $D_x \approx D_{\text{ion}} \approx e^2/R_e \approx e^2/2r_X \approx a_0 \approx IE_X$; $F \approx \Delta^{1/2} \approx 1$; $G \approx 24-30$ and, perhaps also $D_e(\text{XX}) = EA_X$.^[34] So we end ultimately with molecules containing Li (with H or other alkali metals), with BeH bonds and, eventually, with the molecule Li_2 (see for instance Table 4). We had, of course, preferred (*desired*) to end with H_2 to make the analogy between atomic and molecular spectroscopy complete, but maybe this is a matter of further scaling (we refer to the breaking of the $M-Z$ symmetry). In addition, the PE curve generated for Li_2 (ground and excited states) computed from a generalized Kratzer potential coincides with the RKR curve.^[7] Hence, our search for a simple (two-parameter) potential in molecular spectroscopy, brings us back, at least in a first order approximation around R_e , to atomic spectroscopy and the Bohr-atom model. The fact that ionization potentials appear as the leading term in the global molecular scaling process may contribute to this result. Ionization potentials show a well-known Column and Row dependence, as well as a Z and/or mass dependence, capable of transforming the Periodic Table in a one-dimensional array (see our discussion at Figure 1). This is understandable, when looking

at the analytical form of the Kratzer potential, shaped to be applied in atomic spectroscopy too and used by Fermi^[38] in a number of other instances. This now leads to a formal link between atomic and molecular spectroscopy.^[34]

The theoretical basis for the universal character of the Kratzer potential is easily recognized. Its quadratic term in R is a generalization of the quantum hypothesis that the angular momentum be constant or that the velocity of a particle varies as $1/R$. The repulsive part in the Kratzer potential corresponds with a kinetic energy term. This secures that, at equilibrium, the ratio between attraction and repulsion terms is always $1/2$.

Having in mind that Coulomb's law is at the hart of this unifying process and that this fundamental law together with a quantum-hypothesis is automatically included in any Kratzer-type potential, it becomes easier to understand

(a) why a universal potential, if it exists in molecular spectroscopy, is also important for a number of other phenomena in *applied* chemistry^[1]

(b) that such a potential is very suited for scaling spectroscopic constants and, finally,

(c) that a truly universal potential might indeed have exactly this analytical form.

8. Conclusion

We presented almost conclusive evidence that the Holy Grail of Spectroscopy^[10] is an ionic *two-parameter* potential of Kratzer–Varshni–V-type. Bound to a *wrong* asymptote, this simple potential leads to a quantitatively excellent first order approximation for an impressively large number of spectroscopic constants and is superior to a *three-parameter* Morse potential, which uses the *correct* asymptote.

This *wrong* asymptote also gives a smooth picture of the bonding situation at R_e , exactly the only region where Dunham's analysis (which refers to an asymptote of its own) makes sense. Whether or not the best scaling asymptote is the ionic dissociation limit, could be a matter of further research but the present results reveal that it is certainly a good candidate. Hence, ionic asymptotes can no longer be disregarded in *any* theory of chemical bonding.

Even for homonuclear bonding, the accuracy and consistency of the ionic bonding model, which was the standard by excellence in the early days of theoretical chemistry^[6,7,20,21,34] now seems beyond any doubt. Unfortunately, this elementary model was abandoned soon after quantum-mechanical results became available, which led to a new theory of bonding. Ironically enough, exactly the *supposedly poor* performance of ionic potentials in molecular spectroscopy was, at that time, one of the major arguments to abandon the ionic bonding model.^[28] Now, our large-scale analysis shows that, on the contrary, ionic potentials are performing very well. Looking at the situation *near the minimum*, we must conclude that covalent or Lewis bonding can be quantitatively rationalized in terms of ionic bonding, which has its roots in Coulomb's law. The rationale behind the observed simple behavior of spectroscopic constants is

that, *at the minimum*, a bond XX is well represented by an equal mixture of two ionic structures $X^+X^- + X^-X^+$. This gives a different but essentially equivalent interpretation of the Lewis concept of valence electron sharing. It appears that we discovered a *trompe l'oeil* in chemistry^[41]; the *spectroscopic* behavior of *atoms* in *molecules* is rationalized by the interference of an unobservable (*ionic*) *asymptote*, different from the asymptote we can observe: the *atomic dissociation limit*.

Acknowledgments

Spectroscopic work supported by grant G.0073.96 of the FWO-Vlaanderen (Fund for Scientific Research-Flanders).

- [1] J. Ferrante, J. R. Smith, J. H. Rose, *Phys. Rev. Lett.* **1983**, *50*, 1385; J. H. Rose, J. Ferrante, J. R. Smith, *Phys. Rev. Lett.* **1981**, *47*, 675; J. Ferrante, H. Schlosser, J. R. Smith, *Phys. Rev. A*, **1991**, *43*, 3487.
- [2] J. L. Graves, R. G. Parr, *Phys. Rev. A* **1985**, *31*, 1 (see also: J. L. Graves, *Int. J. Quant. Chem.* **1997**, *65*, 1).
- [3] Y. P. Varshni, *Rev. Mod. Phys.* **1957**, *29*(4), 664.
- [4] Y. P. Varshni, R. C. Shukla, *J. Chem. Phys.* **1961**, *35*(2), 582; Y. P. Varshni, R. C. Shukla, *Rev. Mod. Phys.* **1963**, *35*(1), 130; Y. P. Varshni, R. C. Shukla, *J. Molec. Spectr.* **1965**, *16*, 63.
- [5] G. V. Calder, K. Ruedenberg, *J. Chem. Phys.* **1968**, *49*(12), 5399.
- [6] G. Van Hooydonk, *Z. Naturforsch. A* **1982**, *37*, 710; *Z. Naturforsch. A* **1982**, *37*, 971.
- [7] G. Van Hooydonk, *THEOCHEM – J. Mol. Struct.* **1983**, *105*, 69.
- [8] F. Jenc, *Int. Rev. Phys. Chem.* **1996**, *15*(2), 467–523; *Phys. Rev. A*, **1990**, *42*, 403–414; *Adv. At. Mol. Phys.* **1983**, *19*, 265; D. Steele, E. R. Lippincott, J. T. Vanderslice, *Rev. Mod. Phys.* **1968**, *34*, 239.
- [9] K. S. Jhung, I. H. Kim, K. B. Hahn, K.-H. Oh, *Phys. Rev. A*, **1989**, *40*, 7409; K. S. Jhung, I. H. Kim, K.-H. Oh, K. B. Hahn, K. H. C. Jhung, *Phys. Rev. A*, **1990**, *42*, 6497.
- [10] J. Tellinghuisen, S. D. Henderson, D. Austin, K. P. Lawley, R. J. Donovan, *Phys. Rev. A* **1989**, *39*, 925; see also: A. A. Zavitsas, *J. Am. Chem. Soc.* **1991**, *111*, 4755.
- [11] G. B. M. Sutherland, *Proc. Indian Acad. Sci.* **1938**, *8*, 341.
- [12] J. L. Dunham, *Phys. Rev.* **1932**, *41*, 713, 721.
- [13] P. M. Morse, *Phys. Rev.* **1929**, *34*, 57.
- [14] J. R. Smith, H. Schlosser, W. Leaf, J. Ferrante, J. H. Rose, *Phys. Rev. A* **1989**, *39*, 514.
- [15] L. Von Szentpaly, *Chem. Phys. Lett.* **1995**, *245*, 209.
- [16] G. R. Freeman N. H. March, L. Von Szentpaly, *THEOCHEM – J. Mol. Struct.* **1997**, *394*, 11.
- [17] K. P. Huber, G. Herzberg, *Molecular Spectra and Molecular Structure*, vol. IV (Constants of Diatomic Molecules), Van Nostrand-Reinhold, New York, **1979**.
- [18] A. A. Radzig, B. M. Smirnov, *Reference data on atoms, molecules and ions*, Springer Series in Chemical Physics 31, Springer, Berlin, **1985**.
- [19] D. H. Herschbach, V. W. Laurie, *J. Chem. Phys.* **1961**, *35*, 458.
- [20] J. J. Berzelius, *Lehrbuch der Chemie*, Arnold, Dresden, **1835**.
- [21] W. Kossel, *Ann. Phys.* **1916**, *49*, 229; *Z. Phys.* **1924**, *23*, 403.
- [22] R. F. Borkman, R. G. Parr, *J. Chem. Phys.* **1968**, *48*, 1116.
- [23] R. T. Sanderson, *Chemical Bonds and Bond Energy*, Academic Press, New York, **1976**.
- [24] G. Simons, R. G. Parr, J. M. Finlan, *J. Chem. Phys.* **1973**, *59*(6), 3229–3234; G. Simons, J. M. Finlan, *Phys. Rev. Lett.* **1974**, *33*, 131.
- [25] A. Kratzer, *Z. Phys.* **1920**, *3*, 289; *Ann. Phys.* **1922**, *67*, 127.
- [26] M. Born, A. Landé, *Verh. Dsch. Phys. Ges.* **1918**, *20*, 210.
- [27] L. Pauling, *Proc. Nat. Acad. Sci. India* **1956**, *A25*, 1.
- [28] R. S. Mulliken, *Phys. Rev.* **1936**, *50*, 1017; *Phys. Rev.* **1936**, *50*, 1028.
- [29] R. Mecke, *Z. Phys.* **1927**, *42*, 390.
- [30] E. Grüneisen, *Ann. Phys.* **1908**, *26*, 393.
- [31] G. Mie, *Ann. Phys.* **1903**, *11*, 657.
- [32] E. Fues, *Ann. Phys.* **1926**, *80*, 376.
- [33] A. Requena, J. Zuniga, L. M. Fuentes, A. Hidalgo, *J. Chem.*

- Phys.* **1986**, 85, 3939; J. M. Frances, J. Zuniga, M. Alacid, A. Requena, *J. Chem. Phys.* **1989**, 90(10), 5536; A. Bastida, J. Zuniga, M. Alacid, A. Requena, A. Hidalgo, *J. Chem. Phys.* **1990**, 93(5), 3408; A. Requena, M. Alacid, A. Bastida, J. Zuniga, *Int. J. Quant. Chem.* **1994**, 52(1), 165; M. Bag, M. M. Panja, R. Dutt, Y. P. Varshni, *J. Chem. Phys.* **1991**, 95(2), 1139–1143; D. R. Herrick, S. O'Connor, *J. Chem. Phys.* **1998**, 109(6), 2071; R. L. Hall, N. Saad, *J. Chem. Phys.* **1998**, 109(8), 2983; D. Secrest, *J. Chem. Phys.* **1988**, 89, 1017, *J. Phys. Chem.* **1991**, 95(3), 1058; A. Alijah, G. Duxbury, *Mol. Phys.* **1990**, 70(4), 605; J. F. Ogilvie, *J. Chem. Phys.* **1988**, 88(4), 2804; C. Amiot, *J. Chem. Phys.* **1990**, 93(12), 8591, *J. Mol. Spectr.* **1991**, 147(2), 370; B. H. Chang, D. Secrest, *J. Chem. Phys.* **1991**, 84(2), 1196; S. Brajamani, C. A. Singh, *J. Phys. A, Math. Gen.* **1990**, 23(15), 3421; J. Makarewicz, *J. Phys. B, Atom Mol. Opt. Phys.* **1988**, 21(22), 3633; R. E. Moss, I. A. Sadler, *Mol. Phys.* **1989**, 68(5), 1015; M. Molski, J. Konarski, *Phys. Rev. A* **1993**, 47(1), 711, *Chem. Phys. Lett.* **1992**, 196(5), 517, *Acta Phys. Pol. A* **1992**, 81(4–5), 495, *Theor. Chim. Acta* **1993**, 85(5), 325, *J. Molec. Struct.* **1993**, 297, 415; J. Konarski, *Bull. Pol. Acad. Sci. Chem.* **1995**, 43(4), 279; K. Nakagawa, H. Uehara, *Chem. Phys. Lett.* **1990**, 168(1), 96; K. Nakagawa, M. Akiyama, *Chem. Phys. Lett.* **1992**, 190(1–2), 91; J. F. Ogilvie, H. O. Mcc, *J. Molec. Struct.* **1991**, 263, 167; F. M. Fernandez, J. F. Ogilvie, *Chem. Phys. Lett.* **1990**, 169(4), 292; C. G. Diaz, F. M. Fernandez, E. A. Castro, *Chem. Phys.* **1991**, 157(1–2), 35; F. M. Fernandez, E. A. Castro, *J. Math. Chem.* **1993**, 12(1–4), 1; I. L. Cooper, *Chem. Phys.* **1988**, 121(3), 343, *Int. J. Quant. Chem.* **1994**, 49(1), 25; T. Hayes, D. Bellert, T. Buthelezi, P. J. Brucat, *Chem. Phys. Lett.* **1998**, 287(1–2), 22; J. Konarski, *J. Molec. Struct.* **1992**, 270, 491; J. K. G. Watson, *J. Chem. Phys.* **1989**, 90(11), 6443; J. Morales, J. J. Pena, G. Ovando, V. Gaftoi, *J. Math. Chem.* **1997**, 21(3), 273; J. Morales, G. Arreaga, J. J. Pena, V. Gaftoi, G. Ovando, *J. Math. Chem.* **1995**, 18(2–4), 309; K. Tkacz-Smiech, W. S. Ptak, A. Kolezynski, *Int. J. Quant. Chem.* **1996**, 57(6), 1097; K. Tkacz, W. S. Ptak, *J. Molec. Struct.* **1992**, 275, 23; K. Tkacz-Smiech, W. S. Ptak, A. Kolezynski, J. Mrugalski, *Int. J. Quant. Chem.* **1994**, 51(6), 569; K. Tkacz, W. S. Ptak, *THEOCHEM – J. Molec. Struct.* **1989**, 61, 91; P. Chang, C. S. Hsue, *Phys. Rev. A* **1994**, 49(6), 4448; J. Pliva, *J. Molec. Spectr.* **1999**, 193(1), 7; K. A. Walker, M. C. L. Gerry, *J. Chem. Phys.* **1998**, 109(13), 5439; J. Dvorak, L. Skala, *Collect. Czech. Chem. Commun.* **1998**, 63(8), 1161; M. M. Chaudhari, S. H. Behere, *Ind. J. Pure Appl. Phys.* **1996**, 34(1), 42; A. Aguado, J. J. Camacho, M. Paniagua, *THEOCHEM – J. Molec. Struct.* **1992**, 86, 135; Y. Ergun, H. O. Pamuk, E. Yurtsever, *Z. Naturforsch. A* **1990**, 45, 889; C. J. Ballhausen, M. Gajhede, *Chem. Phys. Lett.* **1990**, 165(5), 449; J. Mehra, *Found. Phys.* **1988**, 18(2), 107.
- [34] G. Van Hooydonk, *THEOCHEM – J. Molec. Struct.* **1984**, 109, 87.
- [35] J. K. Wilmshurst, *J. Chem. Phys.* **1959**, 30, 561; *J. Phys. Chem.* **1958**, 62, 631.
- [36] L. Pauling, *J. Am. Chem. Soc.* **1932**, 54, 3570.
- [37] R. S. Mulliken, *J. Chem. Phys.* **1934**, 2, 782.
- [38] V. Weisskopf, *Letters in Theoretical Physics*, vol. III, Interscience, New York, **1961**.
- [39] C. A. Coulson, *Proc. Roy. Soc. (Edinburgh)*, **1932**, A135, 459; L. Pauling, J. Y. Beach, *Phys. Rev.* **1935**, 47, 686.
- [40] D. R. Herrick, S. O'Connor, *J. Chem. Phys.* **1998**, 109(1), 11.
- [41] G. Van Hooydonk, hep-th/9902152 for another application.

Received January 7, 1999
[O99005]